

Towards a complete next-to-logarithmic description of forward exclusive diffractive dijet electroproduction at HERA: real corrections

R. Boussarie

Physics Department, Brookhaven National Laboratory, Upton, NY 11973, USA
Email: rboussarie@bnl.gov

A. V. Grabovsky

Budker Institute of Nuclear Physics, 11, Lavrenteva avenue, 630090, Novosibirsk, Russia &
Novosibirsk State University, 630090, 2, Pirogova street, Novosibirsk, Russia
Email: A.V.Grabovsky@inp.nsk.su

L. Szymanowski

National Centre for Nuclear Research (NCBJ), 02-093 Warsaw, Poland
Email: Lech.Szymanowski@ncbj.gov.pl

S. Wallon

Laboratoire de Physique Théorique (UMR 8627), CNRS, Univ. Paris-Sud, Université Paris-Saclay, 91405, Orsay, France &
Sorbonne Université, Faculté de Physique, 4 place Jussieu, 75252 Paris Cedex 05, France
Email: wallon@th.u-psud.fr

ABSTRACT: We studied the $ep \rightarrow ep+2jets$ diffractive cross section with ZEUS phase space. Neglecting the t -channel momentum in the Born and gluon dipole impact factors, we calculated the corresponding contributions to the cross section differential in $\beta = \frac{Q^2}{Q^2+M_{2jets}^2}$ and the angle ϕ between the leptonic and hadronic planes. The gluon dipole contribution was obtained in the exclusive k_t -algorithm with the exclusive cut $y_{cut} = 0.15$ in the small y_{cut} approximation. In the collinear approximation we canceled singularities between real and virtual contributions to the $q\bar{q}$ dipole configuration, keeping the exact y_{cut} dependency. We used the Golec-Biernat - Wüsthoff (GBW) parametrization for the dipole matrix element and linearized the double dipole contributions. The results give roughly $\frac{1}{2}$ of the observed cross section for small β and coincides with it for large β .

Contents

| | |
|---|-----------|
| 1. Introduction | 1 |
| 2. Kinematics and LO results | 4 |
| 2.1 Leptonic part | 4 |
| 2.2 Hadronic part | 5 |
| 2.3 Experimental cuts | 9 |
| 2.4 BFKL-like approximation | 12 |
| 2.5 Analysis of the LO result | 13 |
| 3. k_t jet algorithm | 15 |
| 3.1 Exclusive k_t jet algorithm for three partons | 15 |
| 3.2 Quark+gluon or antiquark+gluon in one jet | 16 |
| 3.3 Quark+antiquark in one jet | 20 |
| 4. Conclusion | 27 |
| A. Scaling of the aligned versus symmetric jet contributions | 28 |
| B. Dipole-double dipole interference terms | 32 |
| C. Normalization | 33 |

1. Introduction

One of the main outcomes of the HERA research program is the evidence and detailed study of diffractive processes. Indeed, almost 10 % of the $\gamma^*p \rightarrow \text{hadrons}$ deep inelastic scattering (DIS) events were shown to contain a rapidity gap in the detectors between the proton remnants Y and the hadrons X coming from the fragmentation region of the initial virtual photon, namely the process was shown to look like $\gamma^*p \rightarrow XY$. These diffractive deep inelastic scattering (DDIS) events were revealed and extensively studied by H1 and ZEUS collaborations [1–8]. The existence of a rapidity gap between the diffractive state X and the proton remnants, with vacuum quantum numbers in t -channel, is a natural place for a Pomeron-like description. Two types of approaches have been developed.

First, based on the existence of a hard scale (the photon virtuality Q^2 for DIS), a collinear QCD factorization theorem was derived [9] and applied successfully to diffractive processes. For inclusive diffraction, this theorem is usually applied with so-called resolved Pomeron models, where one introduces distributions of partons inside the Pomeron, similarly to the usual parton distribution functions for proton in DIS, convoluted with hard matrix elements. In the framework of collinear factorization diffractive dijet photoproduction was calculated in [10] and [11] in NLO pQCD, where the authors observed collinear factorization breaking. To describe the data it was necessary to introduce a model for the suppression factor or gap survival probability. They demonstrated that a global suppression factor or a model depending on the light cone momentum fraction and the flavour of the interacting parton describe the HERA data. Inclusive dijet photoproduction was also studied in this framework and was shown to be very sensitive to the details of nuclear PDFs in the Pb-Pb ultraperipheral collisions in the LHC kinematics [12], [13].

Second, it is natural at very high energies to view the process as the coupling of a Pomeron with the diffractive state X of invariant mass M . In the rest of this paper, we generically call such descriptions as high-energy factorization pictures. In DDIS case, for low values of M^2 , X can be modeled by a $q\bar{q}$ pair, while for larger values of M^2 , the cross section with an additional produced gluon, i.e. $X = q\bar{q}g$, is enhanced. A good description of HERA data for diffraction was achieved in such a model [14], in which the Pomeron was described by a two-gluon exchange.

In the present paper, we study in detail the cross section for exclusive dijet electroproduction in diffraction, as was recently reported by ZEUS [15]. A first theoretical study of such processes within a high-energy factorization picture was performed in [16], in a leading order (LO) approximation in which the dijet was made of a $q\bar{q}$ pair.

Our aim is to make a description of the same process, relying now on our complete next-to-leading order (NLO) description of the direct coupling of the Pomeron to the diffractive X state, obtained in refs. [17, 18], and further extended to the case of a light vector meson in ref. [19]. In our approach, the Pomeron is understood as a color singlet QCD shockwave, in the spirit of Balitsky's high energy operator expansion [20–23] or in its color glass condensate formulation [24–32].

The exclusive diffractive production of a dijet will be a key process for the physics at the Electron-Ion Collider (EIC) at small x . Indeed, it was proven to probe the dipole Wigner distribution [33]. Several recent studies have been performed in order to build precise target matrix elements for EIC phenomenology [34–36] and for Ultrapерipheral collisions at the LHC [37]. The gluon Wigner distributions probed by our process can describe a cold nuclear origin for elliptic anisotropies, as studied for dilute-dense collisions [38, 39]. Finally the (subeikonal) target spin asymmetry for dijet production was proven to give a direct access to the gluon orbital angular momentum in the target [40, 41]. In this paper, we are interested in building accurate descriptions of the final state via a jet algorithm, to be combined later with the target matrix elements in the aforementioned studies for future precise EIC predictions

We present explicit formulas for Born $ep \rightarrow ep' + 2jets$ cross section allowed by HERA kinematics. We argue that for Born production mechanism, HERA selection cuts for diffractive DIS [15] severely reduce contributions from jets in the aligned configuration since simultaneous restrictions on $p_{\perp jet} > 2$ GeV and $M_{2jets} > 5$ GeV forbid a jet with a very small longitudinal momentum fraction of the photon. As is known [42], the aligned jets give the dominant contribution to the cross section, which in the presently studied kinematics is cut off. Thanks to these cuts the typical transverse energy scale in the Born jet impact factor is greater than the t -channel transverse momentum scale set by the saturation scale Q_s determined by the proton matrix element. As a result, we can expand in the t -channel transverse momentum in the impact factor and analytically take integrals for the γp cross section. This naturally gives the leading power $\sim Q_s^4 \sim W^{2\lambda}$ behavior of the cross section (where $1 + \lambda$ is the pomeron intercept) unlike $\sim Q_s^2 \sim W^\lambda$ for the aligned jets [42] describing large dipoles and saturation. We called this procedure “small Q_s ” or “BFKL-like” approximation.

Next, we study the real radiative corrections. According to the exclusive k_t jet algorithm [43, 44] used in the ZEUS data analysis [15], these corrections come from the $\sim \sqrt{y_{cut}}$ -wide border of the Dalitz plot (see figure 2), with $y_{cut} = 0.15$ being the algorithm parameter. One can symmetrically divide this area into 3 subareas with predominantly $q - (\bar{q}g)$, $\bar{q} - (qg)$, and $g - (q\bar{q})$ jets, where one of the jets is made of $\bar{q}g$, qg , or $q\bar{q}$ correspondingly. At large M_{2jets} the third region gives enhanced contribution since in such kinematics a subdiagram with a t -channel gluon has large $s = M_{2jets}^2$.

Most of the real production matrix elements were calculated in ref. [18] in arbitrary kinematics. We have obtained here the remaining ones and we present them in appendix B. The real production matrix elements have soft and collinear divergencies in the first two regions while the contribution of the third region is finite. Integrating the singular parts over the first two regions, we cancel the singularities with the singular contribution of the virtual part from ref. [18]. As a result, we have the contribution of soft and collinear gluons to the 2 jet cross section in the k_t algorithm. Since the divergent contributions factorize as the Born cross section times the collinear singular factor, the validity criteria of the small Q_s approximation for such contributions are the same as for the Born cross section. Therefore we used this approximation to take the inner integrals in the γp cross section. The average value of this correction is about 10%. However, we noticed that the small y_{cut}

expansion of this contribution is very inaccurate since $\ln^2 y_{cut}$, $\ln y_{cut}$, and the constant contributions together are of the order of the next term $\sim \sqrt{y_{cut}} = 0.39$, which is the true expansion parameter. Although we calculated this contribution exactly in y_{cut} , all other (nonsingular) contributions are $\sim \sqrt{y_{cut}}$ geometrically. Therefore this term alone can not be a good approximation. Instead one can look at it as at a subtraction term for future full numerical calculation.

Among the nonsingular contributions there are ones with the gluon emitted before the shockwave. Suppose for definiteness that it was emitted from the quark and we consider the second, $\bar{q} - (qg)$ region. In such a contribution the invariant mass of the qg pair is small $\sim \sqrt{y_{cut}}$, and the only hard scale in the quark propagator between the photon and the gluon vertices comes from the t -channel. It means that one cannot neglect the t -channel momentum in the impact factor, i.e. the small Q_s approximation is inapplicable. In other words this correction is very sensitive to Q_s . In general, one can say that if one experimentally restricts from below both the mass of the dijet system and the transverse momentum of the jet so that the aligned jets are cut off from the Born cross section, the radiative corrections will greatly depend on saturation effects.

For a generic, roughly symmetric, dijet configuration in the third region with roughly $\frac{1}{2}$ of the photon's longitudinal momentum taken by the gluon and roughly $\frac{1}{4}$ taken by the quark and antiquark each, the typical transverse energy scale in the impact factor is determined by the same parameters as in the Born one: the photon virtuality Q , M_{2jets} , and the experimental cut $p_{\perp jet min}$. Therefore one can also try calculating the contribution of such gluon dipoles in the small Q_s approximation. The validity of this approximation for the configuration when the $(q\bar{q})$ jet itself has the aligned structure is not justified, however, since then the quark or antiquark's part of the longitudinal momentum of the pair becomes a new small parameter. Such a situation happens in the corners of the third $g - (q\bar{q})$ area in the Dalitz plot since in these corners the invariant mass of qg or $\bar{q}g$ becomes small and we return to the situation discussed in the previous paragraph.

Anyway in this paper we have calculated the contribution of all real radiative corrections from the third $g - (q\bar{q})$ area in the Dalitz plot, i.e. the gluon dipole contribution in the small Q_s approximation, i.e. expanding the impact factors in the t -channel momenta. The error of our result comes from the corners of the phase space discussed above and its numerical value will be judged from comparison of our result to the future full numerical calculation. This difference will be related to saturation effects.

This paper is organized as follows. The second part discusses kinematics and yields the LO computation of the cross section, including its leptonic part in section 2.1, hadronic part in section 2.2, HERA acceptance in section 2.3, small Q_s approximation in section 2.4 and analysis of the result in section 2.5. The third part discusses the NLO real corrections including the k_t -jet algorithm in section 3.1, $q - (\bar{q}g)$ and $\bar{q} - (qg)$ dipoles in section 3.2 and $g - (q\bar{q})$ dipole in section 3.3. The conclusion summarizes the paper. Appendix A contains discussion of aligned vs symmetric jet contributions to the Born cross section. Appendix B presents the dipole - double dipole interference impact factors for real correction. Appendix C discusses the overall normalization and matching to non-perturbative distributions in the Golec-Biernat Wüsthoff formulation of DDIS.

2. Kinematics and LO results

2.1 Leptonic part

We will use hereafter the light cone vectors n_1 and n_2 , defined as

$$n_1 \equiv (1, 0_\perp, 1), \quad n_2 \equiv \frac{1}{2}(1, 0_\perp, -1), \quad n_1^+ = n_2^- = (n_1 \cdot n_2) = 1. \quad (2.1)$$

For any vector p we note

$$p^+ = p_- \equiv (p \cdot n_2) = \frac{1}{2}(p^0 + p^3), \quad p_+ = p^- \equiv (p \cdot n_1) = p^0 - p^3, \quad (2.2)$$

$$p = p^+ n_1 + p^- n_2 + p_\perp, \quad (2.3)$$

so that

$$(p \cdot k) = p^\mu k_\mu = p^+ k^- + p^- k^+ + (p_\perp \cdot k_\perp) = p_+ k_- + p_- k_+ - (\vec{p} \cdot \vec{k}). \quad (2.4)$$

The DIS kinematic variables read

$$s = (p_0 + k)^2, \quad q = k - k', \quad Q^2 = -q^2, \quad y = \frac{(p_0 q)}{(p_0 k)} = \frac{W^2 + Q^2}{s}, \quad \bar{y} = 1 - y, \quad (2.5)$$

$$W^2 = (p_0 + q)^2 = 2p_0 q - Q^2, \quad \frac{dk'^+ d^2 k'_\perp}{k'^+} = 2\pi \frac{dW^2 dQ^2}{2s}, \quad (2.6)$$

where p_0, k, k' and q are the proton, initial electron, final electron and photon's momenta and we integrated out the azimuthal angle of the scattered electron w.r.t. the initial electron via overall rotational invariance. The cross section for diffractive dijet production reads

$$d\sigma_{ep} = \frac{4\pi\alpha}{Q^4} J_{\mu\nu} \frac{dk'^+ d^2 k'_\perp}{(2\pi)^3 2k'^+} \frac{I_{\gamma p}}{I_{ep}} d\sigma_{\gamma^* p}^{\mu\nu}. \quad (2.7)$$

Here

$$d\sigma_{\gamma^* p}^{\mu\nu} = M^\mu M^{\nu*} \frac{d\rho_{p,jets}}{4I_{\gamma p}} \quad (2.8)$$

is the γ^* -proton cross section, obtained from the γ^* -proton scattering amplitude M^μ , and

$$\frac{I_{\gamma p}}{I_{ep}} = y, \quad J_{\mu\nu} = \frac{1}{2} \text{tr}(\hat{k} \gamma_\mu \hat{k}' \gamma_\nu) = 2(k_\mu k'_\nu + k'_\mu k_\nu - (kk')g_{\mu\nu}). \quad (2.9)$$

The photon polarization vectors read

$$e^{(0)} = \frac{Q}{(qp_0)} \left(p_0 + \frac{(qp_0)}{Q^2} q \right), \quad e^{(y)} \equiv e^{(-1)} = \frac{n}{\sqrt{-n^2}}, \quad e^{(x)} \equiv e^{(1)} = \frac{\tilde{p}_q}{\sqrt{-\tilde{p}_q^2}}, \quad (2.10)$$

where

$$n_\mu = \varepsilon_{\mu\nu\alpha\beta} p_q^\nu q^\alpha p_0^\beta, \quad \text{and} \quad \tilde{p}_q \equiv p_{q\perp} = p_q - q \left(\frac{(p_0 p_q)}{(p_0 q)} - p_0 \left(\frac{(qp_q)}{(p_0 q)} + \frac{Q^2 (p_0 p_q)}{(p_0 q)^2} \right) \right). \quad (2.11)$$

These polarization vectors obey the identity

$$e_\mu^x e_\nu^{x*} + e_\mu^y e_\nu^{y*} = e_\mu^0 e_\nu^{0*} - g_{\mu\nu} + \frac{q_\mu q_\nu}{q^2}. \quad (2.12)$$

Hereafter, we label the polarizations using Latin indices, while greek letters are used for Lorentz indices. We get

$$J^{ab} = (-1)^{a+b} J^{\mu\nu} e_\mu^{(a)*} e_\nu^{(b)} = 4(-1)^{a+b} (k e^{(a)*})(k e^{(b)}) - (-1)^a Q^2 \delta^{ab}. \quad (2.13)$$

Denoting

$$d\sigma^{ab} = d\sigma_{\gamma^* p}^{\mu\nu} e_\mu^{(a)} e_\nu^{(b)*}, \quad (2.14)$$

we thus have

$$J_{\mu\nu} d\sigma_{\gamma^* p}^{\mu\nu} = J^{ab} d\sigma^{ab}. \quad (2.15)$$

In our light-cone frame

$$p_0 = p_0^- n_2, \quad q = p_\gamma^+ n_1 - \frac{Q^2}{2p_\gamma^+} n_2, \quad W^2 + Q^2 = 2p_0^- p_\gamma^+, \quad (2.16)$$

$$k = p_e^+ n_1 + \frac{\vec{k}^2}{2p_e^+} n_2 + k_\perp, \quad k_\perp^i = |\vec{k}| \begin{pmatrix} \cos \phi \\ \sin \phi \end{pmatrix}, \quad s = 2p_e^+ p_0^-, \quad \vec{k}^2 = \frac{Q^2}{y^2} \bar{y}, \quad (2.17)$$

$$p_q = x p_\gamma^+ n_1 + \frac{\vec{p}_q^2}{2x p_\gamma^+} n_2 + p_{q\perp}, \quad \vec{p}_q^2 = -\vec{p}_q^2, \quad n^2 = -\vec{p}_q^2 \frac{(ys)^2}{4}. \quad (2.18)$$

It is the frame where the photon and the proton are back-to-back, and the z axis is along the direction of the photon momentum. The photoproduction cross section [18] was calculated in this frame. Hence

$$J^{xx} = \frac{2Q^2}{y^2} \left[\bar{y} + \frac{y^2}{2} + \bar{y} \cos(2\phi) \right], \quad J^{00} = \frac{4Q^2}{y^2} \bar{y}, \quad (2.19)$$

$$J^{yy} = \frac{2Q^2}{y^2} \left[\bar{y} + \frac{y^2}{2} - \bar{y} \cos(2\phi) \right], \quad J^{0x} = J^{x0} = \frac{2Q^2}{y^2} (2-y) \sqrt{\bar{y}} \cos \phi, \quad (2.20)$$

and

$$d\sigma_{ep} = \frac{\alpha y}{4\pi} \frac{dW^2 dQ^2}{sQ^4} J^{ab} d\sigma_{\gamma^* p}^{ab}, \quad d\sigma_{\gamma^* p}^{ab} = \frac{d\sigma_{\gamma^* p}^{ab}}{dx d\vec{p}_q d\vec{p}_q} dx d\vec{p}_q d\vec{p}_q. \quad (2.21)$$

2.2 Hadronic part

The density matrix for the cross section in our frame was obtained in (5.21-23) of ref. [18]. To get the proper normalization we have to multiply all cross sections in ref. [18] by $\frac{1}{2(2\pi)^4}$

as is discussed in appendix C. The LO cross sections in our frame read

$$\begin{aligned} \left. \frac{d\sigma_{0TT}^{ij}}{dx d\vec{p}_q d\vec{p}_{\bar{q}}} \right|_{t=0} &= \frac{1}{2(2\pi)^4} \frac{\alpha Q_q^2}{(2\pi)^4 N_c} [((1-2x)^2 - 1)e^{(x)i} e^{(x)j} - g_{\perp}^{ij}] \\ &\times \frac{1}{\vec{p}_{q\bar{q}}^2} \left| \int \frac{d^2 p_{\perp}(\vec{p}_{q\bar{q}}\vec{p})}{\vec{p}^2 + x\bar{x}Q^2} \mathbf{F}(p_{\perp} + \frac{p_{q\bar{q}\perp}}{2}) \right|^2, \end{aligned} \quad (2.22)$$

$$\left. \frac{d\sigma_{0LL}}{dx d\vec{p}_q d\vec{p}_{\bar{q}}} \right|_{t=0} = \frac{1}{2(2\pi)^4} \frac{4\alpha Q_q^2}{(2\pi)^4 N_c} x^2 \bar{x}^2 Q^2 \left| \int \frac{d^2 p_{\perp}}{\vec{p}^2 + x\bar{x}Q^2} \mathbf{F}(p_{\perp} + \frac{p_{q\bar{q}\perp}}{2}) \right|^2, \quad (2.23)$$

$$\begin{aligned} \left. \frac{d\sigma_{0TL}^i e_{i\perp}^{(x)}}{dx d\vec{p}_q d\vec{p}_{\bar{q}}} \right|_{t=0} &= \frac{1}{2(2\pi)^4} \frac{2\alpha_{\text{em}} Q_q^2}{(2\pi)^4 N_c} \frac{x\bar{x}(\bar{x}-x)Q}{\sqrt{\vec{p}_{q\bar{q}}^2}} \int \frac{d^2 \vec{p}_1 \mathbf{F}(p_{1\perp} + \frac{p_{q\bar{q}\perp}}{2})}{\vec{p}_1^2 + x\bar{x}Q^2} \\ &\times \left[\int \frac{d^2 \vec{p}(\vec{p}_{q\bar{q}}\vec{p})}{\vec{p}^2 + x\bar{x}Q^2} \mathbf{F}(p_{\perp} + \frac{p_{q\bar{q}\perp}}{2}) \right]^*, \end{aligned} \quad (2.24)$$

and the total transverse cross section reads

$$\left. \frac{d\sigma_{0TT}}{dx d\vec{p}_q d\vec{p}_{\bar{q}}} \right|_{t=0} = \frac{1}{2} \frac{1}{2(2\pi)^4} \frac{\alpha Q_q^2}{(2\pi)^4 N_c} [(1-2x)^2 + 1] \frac{1}{\vec{p}_{q\bar{q}}^2} \left| \int \frac{d^2 p_{\perp}(\vec{p}_{q\bar{q}}\vec{p})}{\vec{p}^2 + x\bar{x}Q^2} \mathbf{F}(p_{\perp} + \frac{p_{q\bar{q}\perp}}{2}) \right|^2. \quad (2.25)$$

As a result the convolution of the electron tensor and the photon cross section reads

$$J^{ab} \left. \frac{d\sigma_{\gamma^*p}^{ab}}{dx d\vec{p}_q d\vec{p}_{\bar{q}}} \right|_{t=0} = \frac{4Q^2}{y^2} \left[\left. \frac{d\sigma_{0TT}}{dx d\vec{p}_q d\vec{p}_{\bar{q}}} \right|_{t=0} \left\{ \frac{1+\bar{y}^2}{2} - \frac{x\bar{x}}{1-2x\bar{x}} 2\bar{y} \cos(2\phi) \right\} \right] \quad (2.26)$$

$$+ \bar{y} \left. \frac{d\sigma_{0LL}}{dx d\vec{p}_q d\vec{p}_{\bar{q}}} \right|_{t=0} + (2-y) \sqrt{\bar{y}} \cos \phi \left. \frac{d\sigma_{0TL}^i e_{i\perp}^{(x)}}{dx d\vec{p}_q d\vec{p}_{\bar{q}}} \right|_{t=0}. \quad (2.27)$$

Here ϕ is the angle between the quark and the electron's transverse momenta in our frame. Experimentally ϕ is the angle between the jet and the electron, and the jet may come from the antiquark. Then the angle between the quark and the electron is $\pi - \phi$. Therefore one measures the sum of the cross sections with the quark - electron angle equal to ϕ and to $\pi - \phi$. In this sum the interference term σ_{0TL}^i vanishes, σ_{0LL} and σ_{0TT} become twice bigger, and the angle changes from 0 to π . Hence starting from here we will omit the σ_{0TL}^i contribution, understand ϕ as the angle between the jet and the electron, $\phi \in [0, \pi]$, and double σ_{0LL} and σ_{0TT} .

Next, we have to substitute a model for the hadronic matrix elements \mathbf{F} . We will use the Golec-Biernat - Wüsthoff (GBW) [45] parametrization, which was formulated in the coordinate space. To get the proper normalization we Fourier transform (2.23) and compare it with Eq. (4.48) in ref. [42]. Using

$$\frac{1}{\vec{l}^2 + a^2} = \int d^2 r \frac{K_0(ar)}{2\pi} e^{-i\vec{l}\vec{r}}, \quad \mathbf{F}(\vec{k}) = \int d\vec{r} e^{-i\vec{k}\vec{r}} F(\vec{r}), \quad (2.28)$$

we have

$$\left. \frac{d\sigma_{0LL}}{dx d\vec{p}_q d\vec{p}_{\bar{q}}} \right|_{t=0} = \frac{1}{2(2\pi)^4} \frac{4\alpha Q_q^2}{N_c} x^2 \bar{x}^2 Q^2 \left| \int d^2 r \frac{K_0(\sqrt{x\bar{x}}Qr)}{2\pi} e^{i\frac{p_{q\bar{q}\perp}}{2}\vec{r}} F(\vec{r}) \right|^2 \quad (2.29)$$

and

$$\left. \frac{d\sigma_{0LL}}{dt} \right|_{t=0} = \frac{1}{2(2\pi)^4} \frac{4\alpha Q_q^2}{N_c} \pi \int dx Q^2 x^2 \bar{x}^2 \int d^2 r K_0(\sqrt{x\bar{x}} Q r)^2 F(\vec{r})^2. \quad (2.30)$$

Comparing it with (4.48) in ref. [42], the GBW parametrization of the forward dipole matrix element in our normalization reads

$$\begin{aligned} F_{p_{0\perp} p_{0\perp}}(z_\perp) &= \left. \frac{\langle P'(p'_0) | T(\text{tr}(U_{\frac{z_\perp}{2}} U_{-\frac{z_\perp}{2}}^\dagger) - N_c) | P(p_0) \rangle}{2\pi\delta(p_{00'})} \right|_{p_0 \rightarrow p'_0} \\ &= F(z_\perp) = N_c \sigma_0 (1 - e^{-\frac{z_\perp^2}{4R_0^2}}). \end{aligned} \quad (2.31)$$

Here

$$R_0 = \frac{1}{Q_0} \left(\frac{x_P}{a_0} \right)^{\frac{\lambda}{2}}, \quad (2.32)$$

with

$$x_P = \frac{Q^2 + M^2 - t}{Q^2 + W^2}. \quad (2.33)$$

which describes the fraction of the incident momentum lost by the proton or carried by the pomeron. Neglecting the t -channel exchanged momentum, we will write

$$x_P = \frac{Q^2 + M^2}{Q^2 + W^2}. \quad (2.34)$$

In the above model,

$$Q_0 = 1 \text{ GeV}, \quad \sigma_0 = 23.03 \text{ mb}, \quad \lambda = 0.288, \quad a_0 = 3.04 * 10^{-4} \quad (2.35)$$

for 3 active flavours. The nonforward matrix element can be written totally in the impact parameter space

$$F_{p_{0\perp} p_{0'\perp}}(z_\perp) = \int d\vec{b} e^{-i\vec{b}\vec{p}_{0'0}} F_{\vec{b}}(z_\perp). \quad (2.36)$$

Here one can take a simple model [46] that the \vec{b} -dependence factorizes into a Gaussian proton profile

$$F_{\vec{b}}(z_\perp) = \frac{1}{2\pi B_G} e^{-\frac{b^2}{2B_G}} F_0(z_\perp) = \frac{1}{2\pi B_G} e^{-\frac{b^2}{2B_G}} N_c \sigma_0 (1 - e^{-\frac{z_\perp^2}{4R_0^2}}) \quad (2.37)$$

with

$$B_G = 4 \text{ GeV}^{-2}. \quad (2.38)$$

We will need this function in the momentum space

$$\begin{aligned} \mathbf{F}_{p_{0\perp} p_{0'\perp}}(p_\perp) &= \int d\vec{z} e^{-i\vec{z}\vec{p}} \int d\vec{b} e^{-i\vec{b}\vec{p}_{0'0}} F_{\vec{b}}(z_\perp) \\ &= N_c \sigma_0 \left[(2\pi)^2 \delta(\vec{p}) - 4\pi R_0^2 e^{-R_0^2 \vec{p}^2} \right] e^{-\frac{B_G}{2} \vec{p}_{0'0}^2} = \mathbf{F}(p_\perp) e^{-\frac{B_G}{2} \vec{p}^2}, \end{aligned} \quad (2.39)$$

with

$$\vec{\tau} = \vec{p}_q + \vec{p}_{\bar{q}}. \quad (2.40)$$

Therefore in (2.23) and (2.25)

$$\mathbf{F}(p_{\perp}) = (2\pi)^2 N_c \sigma_0 \left[\delta(\vec{p}) - \frac{R_0^2}{\pi} e^{-R_0^2 \vec{p}^2} \right]. \quad (2.41)$$

Denoting

$$\vec{M} = \sqrt{x\bar{x}} \left(\frac{\vec{p}_q}{x} - \frac{\vec{p}_{\bar{q}}}{\bar{x}} \right), \quad (2.42)$$

we thus have

$$\frac{\partial(\vec{M}, \vec{\tau})}{\partial(\vec{p}_q, \vec{p}_{\bar{q}})} = \frac{1}{x\bar{x}}, \quad (2.43)$$

and

$$\vec{p}_q = x\vec{\tau} + \sqrt{x\bar{x}} \vec{M}, \quad \vec{p}_{\bar{q}} = \bar{x}\vec{\tau} - \sqrt{x\bar{x}} \vec{M}, \quad \vec{p}_{q\bar{q}} = (x - \bar{x})\vec{\tau} + 2\sqrt{x\bar{x}} \vec{M}. \quad (2.44)$$

One then gets

$$dx d\vec{p}_q d\vec{p}_{\bar{q}} = x\bar{x} dx d\vec{M} d\vec{\tau} = x\bar{x} dx \frac{dM^2}{2} d\phi \frac{d\tau^2}{2} d\phi_{\tau} = \frac{\pi}{2B_G} x\bar{x} dx dM^2 d\phi. \quad (2.45)$$

Here ϕ is the relative angle between the jet and leptonic planes. It is useful to introduce the Bjorken variable β normalized to the pomeron momentum, which reads

$$\beta = \frac{Q^2}{Q^2 + M^2 - t}. \quad (2.46)$$

Neglecting the t -channel exchanged momentum (experimentally, t could not be measured in ZEUS analysis, but was presumably rather small), we will use the simplified expression

$$\beta = \frac{Q^2}{Q^2 + M^2}, \quad (2.47)$$

and thus, denoting $\bar{\beta} = 1 - \beta$,

$$M^2 = Q^2 \frac{\bar{\beta}}{\beta}. \quad (2.48)$$

We need the differential cross section in x , β and ϕ . From

$$\frac{dM^2}{d\beta} = -\frac{Q^2}{\beta^2}, \quad (2.49)$$

we thus have

$$dx d\vec{p}_q d\vec{p}_{\bar{q}} \rightarrow \frac{Q^2 \pi}{2\beta^2 B_G} x\bar{x} dx d\beta d\phi. \quad (2.50)$$

2.3 Experimental cuts

We will now consider the experimental set-up of the ZEUS collaboration. The HERA kinematics is such that $E_{e^-} = 27.5$ GeV and $E_p = 920$ GeV, i.e. $\sqrt{s} = 318$ GeV. The phase space covered by the ZEUS collaboration reads [15]

$$W_{\min} = 90 \text{ GeV} < W < W_{\max} = 250 \text{ GeV}, \quad Q_{\min} = 5 \text{ GeV} < Q, \quad (2.51)$$

$$M_{\min} = 5 \text{ GeV} < M, \quad x_P < x_{P_{\max}} = 0.01. \quad (2.52)$$

Hence, using eq. (2.34) one has

$$M^2 < x_{P_{\max}} W^2 - Q^2(1 - x_{P_{\max}}). \quad (2.53)$$

For fixed β we have, using eq. (2.48),

$$\max\left(Q_{\min}^2, \frac{\beta}{\beta} M_{\min}^2\right) < Q^2 < \frac{x_{P_{\max}} \beta}{1 - x_{P_{\max}} \beta} W^2. \quad (2.54)$$

A careful study shows that

$$\beta_{\min} = \frac{Q_{\min}^2}{x_{P_{\max}}(W_{\max}^2 + Q_{\min}^2)}, \quad \beta_{\max} = \frac{W_{\max}^2 x_{P_{\max}} - M_{\min}^2}{x_{P_{\max}}(W_{\max}^2 - M_{\min}^2)}. \quad (2.55)$$

On the other hand, eq. (2.54) leads to

$$\max\left[W_{\min}^2, \max\left(Q_{\min}^2, M_{\min}^2 \frac{\beta}{\beta}\right) \frac{1 - x_{P_{\max}} \beta}{x_{P_{\max}} \beta}\right] < W^2 < W_{\max}^2. \quad (2.56)$$

The inelasticity restriction reads

$$y_{\min} = 0.1 < y < y_{\max} = 0.65, \quad \text{i.e.} \quad y_{\min} s < Q^2 + W^2 < y_{\max} s. \quad (2.57)$$

Eqs. (2.54) and (2.57) thus result in the following constraints for Q^2 :

$$\max\left(Q_{\min}^2, M_{\min}^2 \frac{\beta}{\beta}, y_{\min} s - W^2\right) < Q^2 < \min\left(\frac{x_{P_{\max}} \beta}{1 - x_{P_{\max}} \beta} W^2, y_{\max} s - W^2\right) \quad (2.58)$$

One should note that in eq. (2.58),

$$\min\left(\frac{x_{P_{\max}} \beta}{1 - x_{P_{\max}} \beta} W^2, y_{\max} s - W^2\right) = y_{\max} s - W^2 \quad (2.59)$$

would mean that

$$\frac{1}{x_{P_{\max}}} \left(1 - \frac{W^2}{y_{\max} s}\right) < \beta < \beta_{\max} \quad (2.60)$$

and thus, using the expression of β_{\max} , see eq. (2.55), that

$$y_{\max} s < W_{\max}^2 + Q_{\min}^2. \quad (2.61)$$

For the experimental values of ZEUS, this is not satisfied, and one can thus simplify the constraints (2.58) on Q^2 as

$$\max\left(Q_{\min}^2, M_{\min}^2 \frac{\beta}{\beta}, y_{\min} s - W^2\right) < Q^2 < \frac{x_{P_{\max}} \beta}{1 - x_{P_{\max}} \beta} W^2. \quad (2.62)$$

Similarly, Eqs. (2.54) and (2.57) result in the following constraints for W^2 :

$$(1 - x_{P\max}\beta) \max\left(y_{\min}s, \frac{Q_{\min}^2}{x_{P\max}\beta}, \frac{M_{\min}^2}{x_{P\max}\bar{\beta}}\right) < W^2 < W_{\max}^2. \quad (2.63)$$

Additionally, there is a restriction on the transverse momentum of the jet

$$p > p_{\min} = 2 \text{ GeV}. \quad (2.64)$$

In the $t = 0$ limit, i.e. $\vec{\tau} = \vec{0}$, we have from eq. (2.44) $p = |\vec{p}_q| = |\vec{p}_{\bar{q}}| = \sqrt{x\bar{x}}M$. Thus, the constraint (2.64) reads

$$p^2 = x\bar{x}M^2 = x\bar{x}\frac{\bar{\beta}}{\beta}Q^2 > p_{\min}^2 \quad (2.65)$$

and leads to the following restrictions on x :

$$x \in [x_{\min}, \bar{x}_{\min}] \equiv \left[\frac{1}{2} - \sqrt{\frac{1}{4} - \frac{p_{\min}^2\beta}{Q^2\bar{\beta}}}, \frac{1}{2} + \sqrt{\frac{1}{4} - \frac{p_{\min}^2\beta}{Q^2\bar{\beta}}}\right]. \quad (2.66)$$

There is one more experimental cut imposed in ref. [15]. It is the restriction on the jet rapidity $\eta_{\max} = 2$, where the rapidity is defined in the detector frame with the z axis along the proton and electron velocities in the proton beam direction. One can rewrite this cut as cut on x_{\min} as well. Indeed, one can transform momenta from the proton-photon frame (2.16–2.18) to the detector frame. For any vector l

$$l_{Det} = R_{xz}\Lambda_x R_{xy}\Lambda_z l, \quad (2.67)$$

$$\Lambda : l^+ \rightarrow \lambda l^+, l^- \rightarrow \frac{1}{\lambda} l^-, \quad R_{xy} = \begin{pmatrix} 1 & & & \\ & \cos \phi & \sin \phi & \\ & -\sin \phi & \cos \phi & \\ & & & 1 \end{pmatrix}, \quad (2.68)$$

$$\Lambda_x = \begin{pmatrix} \gamma & \beta\gamma & & \\ \beta\gamma & \gamma & & \\ & & 1 & \\ & & & 1 \end{pmatrix}, \quad R_{xz} = \begin{pmatrix} 1 & & & \\ & \cos \alpha & -\sin \alpha & \\ & & 1 & \\ & \sin \alpha & \cos \alpha & \end{pmatrix}, \quad (2.69)$$

where

$$\beta = -\sin \alpha, \quad \gamma = \frac{1}{\cos \alpha}, \quad \sin \alpha = \frac{k}{2\lambda p_e^+}. \quad (2.70)$$

After this transformation one gets

$$p_{0Det} = \frac{sy}{\sqrt{(2\lambda y p_e^+)^2 - Q^2 \bar{y}}} n_2, \quad k_{Det} = \frac{1}{2y} \sqrt{(2\lambda y p_e^+)^2 - Q^2 \bar{y}} n_1, \quad (2.71)$$

$$q_{Det} = \frac{1}{2} \sqrt{(2\lambda y p_e^+)^2 - Q^2 \bar{y}} n_1 - \frac{Q^2 y}{\sqrt{(2\lambda y p_e^+)^2 - Q^2 \bar{y}}} n_2 - Q \sqrt{\bar{y}} e_{x\perp}, \quad (2.72)$$

$$p_{qDet} = \frac{x}{2} \sqrt{(2\lambda y p_e^+)^2 - Q^2 \bar{y}} n_1 + \frac{\vec{p}_q^2 - 2x p_q Q \sqrt{\bar{y}} \cos \phi + Q^2 x^2 \bar{y}}{x \sqrt{(2\lambda y p_e^+)^2 - Q^2 \bar{y}}} \\ + (p_q \cos \phi - Q x \sqrt{\bar{y}}) e_{x\perp} - p_q \sin \phi e_{y\perp}. \quad (2.73)$$

In the detector frame

$$k_{Det}^+ = \frac{1}{2y} \sqrt{(2\lambda y p_e^+)^2 - Q^2 \bar{y}} = E_e = 27.5 \text{ GeV}. \quad (2.74)$$

This condition fixes p_e^+ or λ , the remaining parameter representing freedom in z -boosts in the γ -proton frame. Then p_{qDet} 's rapidity reads

$$\eta_{qDet} = \frac{1}{2} \ln \frac{4E_e^2 x^2 y^2}{\bar{p}_q^2 - 2xp_q Q \sqrt{\bar{y}} \cos \phi + Q^2 x^2 \bar{y}} > -\eta_{\max}, \quad (2.75)$$

where we changed the sign to take into account the propagation along the negative z direction (the z axis in the ZEUS frame and in our frame are opposite). Obviously, this constraint should be fulfilled for both quark and the antiquark jets, i.e. eq. (2.75) with $x \rightarrow \bar{x}$. A careful inspection then shows that these two constraints turn into

$$\begin{aligned} x, \bar{x} > x_0 = \bar{\beta} \quad (2.76) \\ \beta \left(\frac{2E_e y}{Q} \right)^2 - 2\beta e^{-\eta_{\max}} \cos \phi \sqrt{\bar{y} \left(\left(\frac{2E_e y}{Q} \right)^2 - e^{-2\eta_{\max}} \bar{y} \sin^2 \phi \right)} + e^{-2\eta_{\max}} (\bar{\beta} + \beta \bar{y} \cos(2\phi)) \\ \times \frac{2\beta \bar{y} \left(e^{-2\eta_{\max}} \bar{\beta} \cos(2\phi) - \beta \left(\frac{2E_e y}{Q} \right)^2 \right) + e^{2\eta_{\max}} \left(e^{-2\eta_{\max}} \bar{\beta} + \beta \left(\frac{2E_e y}{Q} \right)^2 \right)^2 + \beta^2 e^{-2\eta_{\max}} \bar{y}^2}{2\beta \bar{y} \left(e^{-2\eta_{\max}} \bar{\beta} \cos(2\phi) - \beta \left(\frac{2E_e y}{Q} \right)^2 \right) + e^{2\eta_{\max}} \left(e^{-2\eta_{\max}} \bar{\beta} + \beta \left(\frac{2E_e y}{Q} \right)^2 \right)^2 + \beta^2 e^{-2\eta_{\max}} \bar{y}^2}. \end{aligned}$$

The minimal value for x is thus

$$\tilde{x}_{\min} = \max(x_{\min}, x_0), \quad (2.77)$$

with the additional constraint that $\tilde{x}_{\min} < \frac{1}{2}$. However as we will show later, numerically this rapidity restriction is negligible. Therefore we will include it only in the discussion of the final result.

Finally, one has to calculate

$$\begin{aligned} \frac{d\sigma_{ep}}{d\beta d\phi} = 2 \frac{\alpha}{\beta^2 B_G} \int_{(1-x_{P_{\max}\beta})}^{W_{\max}^2} \max\left(y_{\min s}, \frac{Q_{\min}^2}{x_{P_{\max}\beta}}, \frac{M_{\min}^2}{x_{P_{\max}\beta}}\right) \frac{dW^2}{2s} \int_{\max(Q_{\min}^2, M_{\min}^2 \frac{\beta}{\bar{\beta}}, y_{\min s} - W^2)}^{\frac{x_{P_{\max}\beta}}{1-x_{P_{\max}\beta}} W^2} \frac{dQ^2}{y} \\ \times \int_{x_{\min}}^{\tilde{x}_{\min}} x \bar{x} dx \left[\bar{y} \left. \frac{d\sigma_{0LL}}{dx d\vec{p}_q d\vec{p}_{\bar{q}}} \right|_{t=0} + \left. \frac{d\sigma_{0TT}}{dx d\vec{p}_q d\vec{p}_{\bar{q}}} \right|_{t=0} \left\{ \frac{1 + \bar{y}^2}{2} - \frac{2\bar{y}x\bar{x}}{1 - 2x\bar{x}} \cos(2\phi) \right\} \right], \quad (2.78) \end{aligned}$$

where $\phi \in [0, \pi]$ and

$$\left. \frac{d\sigma_{0LL}}{dx d\vec{p}_q d\vec{p}_{\bar{q}}} \right|_{t=0} = \frac{1}{(\hbar c)^2} \frac{1}{2(2\pi)^4} \frac{4\alpha Q_q^2}{(2\pi)^4 N_c} x^2 \bar{x}^2 Q^2 \left| \int \frac{d^2 p_{\perp}}{\vec{p}^2 + x\bar{x}Q^2} \mathbf{F}\left(p_{\perp} + \frac{p_{q\bar{q}\perp}}{2}\right) \right|^2, \quad (2.79)$$

$$\left. \frac{d\sigma_{0TT}}{dx d\vec{p}_q d\vec{p}_{\bar{q}}} \right|_{t=0} = \frac{1}{(\hbar c)^2} \frac{1}{2(2\pi)^4} \frac{1}{2} \frac{\alpha Q_q^2}{(2\pi)^4 N_c} [(1 - 2x)^2 + 1] \frac{1}{\bar{p}_{q\bar{q}}^2} \left| \int \frac{d^2 p_{\perp} (\vec{p}_{q\bar{q}} \vec{p})}{\vec{p}^2 + x\bar{x}Q^2} \mathbf{F}\left(p_{\perp} + \frac{p_{q\bar{q}\perp}}{2}\right) \right|^2, \quad (2.80)$$

with

$$\vec{p}_{q\bar{q}} = 2\sqrt{x\bar{x}m} \vec{e}^{(x)} = 2\sqrt{x\bar{x}} \frac{\bar{\beta}}{\beta} Q \vec{e}^{(x)}, \quad (2.81)$$

$$\mathbf{F}(p_\perp) = (2\pi)^2 N_c \sigma_0 \left[\delta(\vec{p}) - \frac{R_0^2}{\pi} e^{-R_0^2 \vec{p}^2} \right] = -(2\pi)^2 \frac{N_c \sigma_0}{\pi} e^{-R_0^2 \vec{p}^2} \frac{\partial}{\partial p^2}. \quad (2.82)$$

The t -channel integrals can be simplified

$$\int \frac{d^2 p_\perp}{\vec{p}^2 + x\bar{x}Q^2} \mathbf{F}(p_\perp + \frac{p_{q\bar{q}\perp}}{2}) = \int_0^{+\infty} \frac{\pi \mathbf{F}(p) dp^2}{\sqrt{(x\bar{x}Q^2 + p^2 + (\frac{\vec{p}_{q\bar{q}}}{2})^2)^2 - 4p^2(\frac{\vec{p}_{q\bar{q}}}{2})^2}} \quad (2.83)$$

$$= -N_c \sigma_0 \int_0^{+\infty} dp^2 e^{-R_0^2 \vec{p}^2} \frac{\partial}{\partial p^2} \frac{(2\pi)^2}{\sqrt{(x\bar{x}Q^2 + p^2 + (\frac{\vec{p}_{q\bar{q}}}{2})^2)^2 - 4p^2(\frac{\vec{p}_{q\bar{q}}}{2})^2}}, \quad (2.84)$$

$$\frac{1}{|\vec{p}_{q\bar{q}}|} \int \frac{d^2 p_\perp (\vec{p}_{q\bar{q}} \vec{p})}{\vec{p}^2 + x\bar{x}Q^2} \mathbf{F}(p_\perp + \frac{p_{q\bar{q}\perp}}{2}) = \int_0^{+\infty} \frac{dp^2}{2} \mathbf{F}(p) \int d\phi \frac{(\vec{e}^{(x)}, \vec{p} - \frac{\vec{p}_{q\bar{q}}}{2})}{(\vec{p} - \frac{\vec{p}_{q\bar{q}}}{2})^2 + x\bar{x}Q^2} \quad (2.85)$$

$$= \pi \int_0^{+\infty} dp^2 \frac{\mathbf{F}(p)}{2 \frac{|\vec{p}_{q\bar{q}}|}{2}} \left(\frac{x\bar{x}Q^2 + p^2 - (\frac{\vec{p}_{q\bar{q}}}{2})^2}{\sqrt{(x\bar{x}Q^2 + p^2 + (\frac{\vec{p}_{q\bar{q}}}{2})^2)^2 - 4p^2(\frac{\vec{p}_{q\bar{q}}}{2})^2}} - 1 \right) \quad (2.86)$$

$$= -(2\pi)^2 \frac{N_c \sigma_0}{2 \frac{|\vec{p}_{q\bar{q}}|}{2}} \int_0^{+\infty} dp^2 e^{-R_0^2 \vec{p}^2} \frac{\partial}{\partial p^2} \frac{x\bar{x}Q^2 + p^2 - (\frac{\vec{p}_{q\bar{q}}}{2})^2}{\sqrt{(x\bar{x}Q^2 + p^2 + (\frac{\vec{p}_{q\bar{q}}}{2})^2)^2 - 4p^2(\frac{\vec{p}_{q\bar{q}}}{2})^2}}. \quad (2.87)$$

These integrals will be calculated numerically.

2.4 BFKL-like approximation

In our kinematics the saturation scale is much lower than all other scales. Indeed, we have

$$\frac{Q_{\min}^2 + M_{\min}^2}{Q_{\min}^2 + W_{\max}^2} \simeq 0.0008 < x_P < 0.01, \quad (2.88)$$

$$Q_s^2 = \frac{1}{R_0^2} < 0.8 \text{ GeV}^2 < p_{\min}^2 = 2^2 \text{ GeV}^2 \ll Q^2, M^2 \in [5^2, 25^2] \text{ GeV}^2. \quad (2.89)$$

It means that neglecting p^2 in the denominator in (2.87) gives the error

$$\sim \left| \frac{2p^2(x\bar{x}Q^2 - (\frac{\vec{p}_{q\bar{q}}}{2})^2)}{(x\bar{x}Q^2 + (\frac{\vec{p}_{q\bar{q}}}{2})^2)^2} \right| \leq \frac{2p^2}{x\bar{x}Q^2 + p_{\min}^2}. \quad (2.90)$$

Therefore at least with $O(\frac{Q_s^2}{p_{\min}^2})$ precision one can neglect the t -channel momentum in the integrals and calculate them analytically to get

$$\begin{aligned} \int \frac{d^2 p_\perp}{\vec{p}^2 + x\bar{x}Q^2} \mathbf{F}(p_\perp + \frac{p_{q\bar{q}\perp}}{2}) &\simeq -(2\pi)^2 \frac{N_c \sigma_0}{R_0^2} \frac{(\frac{\vec{p}_{q\bar{q}}}{2})^2 - x\bar{x}Q^2}{((\frac{\vec{p}_{q\bar{q}}}{2})^2 + x\bar{x}Q^2)^3} \\ &= -\frac{(2\pi)^2 N_c \sigma_0}{R_0^2 (x\bar{x})^2} \frac{M^2 - Q^2}{(M^2 + Q^2)^3} = -(2\pi)^2 \frac{N_c \sigma_0 (\bar{\beta} - \beta) \beta^2}{Q^4 R_0^2 (x\bar{x})^2}, \end{aligned} \quad (2.91)$$

and

$$\begin{aligned}
& \int \frac{d^2 p_\perp (\vec{p}_{q\bar{q}} \vec{p})}{\vec{p}^2 + x\bar{x}Q^2} \frac{\mathbf{F}(p_\perp + \frac{p_{q\bar{q}\perp}}{2})}{|\vec{p}_{q\bar{q}}|} \simeq -\frac{N_c \sigma_0}{R_0^2} \frac{(2\pi)^2 2 \frac{|\vec{p}_{q\bar{q}}|}{2} x\bar{x}Q^2}{((\frac{\vec{p}_{q\bar{q}}}{2})^2 + x\bar{x}Q^2)^3} \\
& = -\frac{(2\pi)^2 N_c \sigma_0}{R_0^2 (x\bar{x})^{\frac{3}{2}}} \frac{2mQ^2}{(M^2 + Q^2)^3} = -(2\pi)^2 \frac{N_c \sigma_0 2\sqrt{\beta}\beta^{\frac{5}{2}}}{Q^3 R_0^2 (x\bar{x})^{\frac{3}{2}}}.
\end{aligned} \tag{2.92}$$

In this approximation the ep cross section (2.78) reads

$$\begin{aligned}
\left. \frac{d\sigma_{ep}}{d\beta d\phi} \right|_{\text{Born}} &= \frac{2\alpha^2 Q_q^2 N_c \sigma_0^2}{(2\pi)^4 B_G (\hbar c)^2} \int_{(1-x_{P\max\beta})\max(y_{\min s}, \frac{Q_{\min}^2}{x_{P\max\beta}}, \frac{M_{\min}^2}{x_{P\max\beta}})}^{W_{\max}^2} \frac{dW^2}{s} \\
&\times \int_{\max(Q_{\min}^2, M_{\min}^2 \frac{\beta}{\beta}, y_{\min s} - W^2)}^{\frac{x_{P\max\beta}}{1-x_{P\max\beta}} W^2} \frac{dQ^2}{y R_0^4 Q^6} \\
&\times \int_{x_{\min}}^{\bar{x}_{\min}} dx \left[\bar{y} \frac{(\bar{\beta} - \beta)^2 \beta^2}{x\bar{x}} + \frac{[(1-2x)^2 + 1]}{2} \frac{\bar{\beta}\beta^3}{(x\bar{x})^2} \left\{ \frac{1 + \bar{y}^2}{2} - \frac{2\bar{y}x\bar{x}}{1-2x\bar{x}} \cos(2\phi) \right\} \right].
\end{aligned} \tag{2.93}$$

Then the integral w.r.t. x can be performed analytically

$$\begin{aligned}
\left. \frac{d\sigma_{ep}}{d\beta d\phi} \right|_{\text{Born}} &= \frac{4\alpha^2 Q_q^2 N_c \sigma_0^2}{(2\pi)^4 B_G (\hbar c)^2} \int_{(1-x_{P\max\beta})\max(y_{\min s}, \frac{Q_{\min}^2}{x_{P\max\beta}}, \frac{M_{\min}^2}{x_{P\max\beta}})}^{W_{\max}^2} \frac{dW^2}{s} \\
&\times \int_{\max(Q_{\min}^2, M_{\min}^2 \frac{\beta}{\beta}, y_{\min s} - W^2)}^{\frac{x_{P\max\beta}}{1-x_{P\max\beta}} W^2} \frac{dQ^2}{y R_0^4 Q^6} \\
&\times \left[\bar{y} (\bar{\beta} - \beta)^2 \beta^2 \ln \left(\frac{\bar{x}_{\min}}{x_{\min}} \right) + \bar{\beta}\beta^3 \left\{ \frac{1 + \bar{y}^2}{2} \frac{1 - 2x_{\min}}{x_{\min}\bar{x}_{\min}} - 2\bar{y} \ln \left(\frac{\bar{x}_{\min}}{x_{\min}} \right) \cos(2\phi) \right\} \right].
\end{aligned} \tag{2.94}$$

The results integrated w.r.t. $\phi \in [0, \pi]$ are in figure 1. As one can see the approximation errors are smaller than the experimental ones.

2.5 Analysis of the LO result

Following ref. [42], we rewrite (2.94) in terms of diffractive structure functions F^D . These functions are defined through

$$\frac{d\sigma_{ep}}{dx_B dQ^2 dx_P dt} = \frac{4\pi\alpha^2}{x_B Q^4} \left\{ \frac{1 + \bar{y}^2}{2} F_T^{D(4)} + \bar{y} F_L^{D(4)} \right\}, \tag{2.95}$$

$$F_{T,L}^{D(4)}(x_B, Q^2, x_P, t) = \frac{dF_{T,L}^D}{dx_P dt} = \frac{Q^2}{4\pi^2 \alpha} \frac{d\sigma_{T,L}^{\gamma p}}{dx_P dt}, \quad F_{T,L}^{D(3)} = \int_{-\infty}^0 dt F_{T,L}^{D(4)}, \tag{2.96}$$

where

$$x_B = \frac{Q^2}{2p_{0q}} = \frac{Q^2}{W^2 + Q^2} = \beta x_P \tag{2.97}$$

is the Bjorken variable. Since

$$dx_B = -\frac{x_B^2}{Q^2} dW^2, \quad dx_P = -x_P \frac{d\beta}{\beta}, \tag{2.98}$$

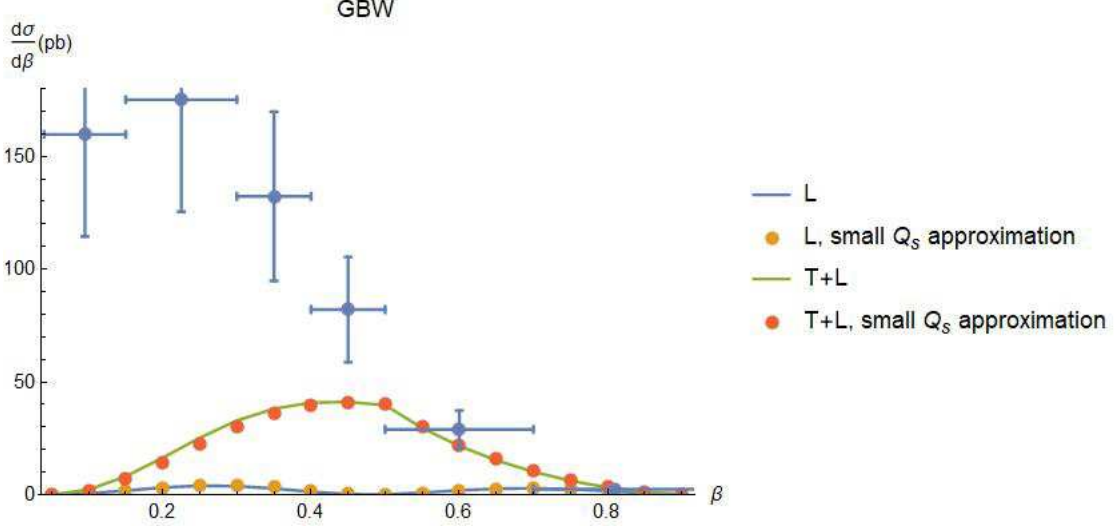


Figure 1: Longitudinal (L) and both transverse and longitudinal photon contributions to the dijet cross section calculated exactly from LO formulas (2.84-2.87) and in the small Q_s approximation (2.91-2.92).

one gets

$$x_P F_T^{D(3)} = \frac{Q_q^2 N_c \sigma_0^2}{(2\pi)^4 B_G (\hbar c)^2} \frac{\bar{\beta} \beta^4}{Q^2 R_0^4} \frac{1 - 2x_{\min}}{x_{\min} \bar{x}_{\min}}, \quad (2.99)$$

$$x_P F_L^{D(3)} = \frac{Q_q^2 N_c \sigma_0^2}{(2\pi)^4 B_G (\hbar c)^2} \frac{(\bar{\beta} - \beta)^2 \beta^3}{Q^2 R_0^4} \ln \left(\frac{\bar{x}_{\min}}{x_{\min}} \right), \quad (2.100)$$

which gives in the small β ($M^2 \gg Q^2$) region

$$x_P F_T^{D(3)} \simeq \frac{\sigma_0^2}{B_G} \frac{\beta^4}{Q^2 R_0^4 p_{\min}^2 \beta}, \quad x_P F_L^{D(3)} \simeq \frac{\sigma_0^2}{B_G} \frac{\beta^3}{Q^2 R_0^4} \ln \left(\frac{Q^2}{p_{\min}^2 \beta} \right). \quad (2.101)$$

This behavior contradicts the known one [42]

$$x_P \tilde{F}_T^{D(3)} \sim \frac{\sigma_0^2 \beta \bar{\beta}}{B_G R_0^2}, \quad x_P \tilde{F}_L^{D(3)} \sim \frac{\sigma_0^2}{B_G} \frac{\beta^3}{Q^2 R_0^4}, \quad (2.102)$$

where we introduced \tilde{F} to distinguish them from our result.

First, let us emphasize that our transverse structure function $F_T^{D(3)}$ is correctly proportional to $\bar{\beta}$. Indeed, since the final $q\bar{q}$ pair has opposite helicities, it carries angular momentum as orbital momentum and its wave function scales like $p_{\perp} \sim M$. Therefore it should vanish at $M = 0$, i.e. $\beta = 1$.

Next, $F_T^{D(3)}$ is a higher twist correction compared to (2.102) as it has an extra power of $Q^2 R_0^2 \gg 1$ in its denominator. The origin of this suppression lies in the fact that the dominant contribution to the transverse cross section comes from the aligned jet configuration, i.e. the region of $x \lesssim \frac{1}{\max(Q^2, M^2) R_0^2} \ll 1$. We discuss it in Appendix A. However in our kinematics (2.66), (2.88-2.89)

$$\frac{1}{M^2 R_0^2} < \frac{0.8 \text{ GeV}^2}{M^2} \ll x_{\min} = \frac{1}{2} - \sqrt{\frac{1}{4} - \frac{4 \text{ GeV}^2}{M^2}}, \quad (2.103)$$

which for the largest $M^2 \simeq 25^2 \text{ GeV}^2$ gives

$$\frac{1}{M^2 R_0^2} \simeq 0.001 \ll x_{\min} \simeq 0.006. \quad (2.104)$$

Therefore the current experimental setup does not let us probe the leading twist contribution to the transverse cross section. In other words the experimental cuts kill the leading twist aligned jets which come from the saturation region. As a result we are left with the subleading twist perturbative BFKL-like ($\sigma \sim s^{2\lambda}$) behavior (2.94). One can also feel that the experiment sees only the subleading twist contribution from fig. 6d in ref. [15] where they cut off the p_\perp distribution peak.

The longitudinal structure function is subleading to the transverse one in twist (2.102). The whole $0 < x < 1$ range contributes to it. Therefore the experimental cuts only change the β -dependence of the result.

3. k_t jet algorithm

3.1 Exclusive k_t jet algorithm for three partons

Let us recall the parametrization of the momenta of the 3 outgoing partons. For the 3 particles with the momenta

$$p_q = x_q p_\gamma^+ n_1 + \frac{\vec{p}_q^2}{2x_q p_\gamma^+} n_2 + p_{q\perp}, \quad p_{\bar{q}} = x_{\bar{q}} p_\gamma^+ n_1 + \frac{\vec{p}_{\bar{q}}^2}{2x_{\bar{q}} p_\gamma^+} n_2 + p_{\bar{q}\perp}, \quad (3.1)$$

$$p_g = z p_\gamma^+ n_1 + \frac{\vec{p}_g^2}{2z p_\gamma^+} n_2 + p_{g\perp}, \quad p = p_q + p_{\bar{q}} + p_g, \quad M^2 = p^2, \quad (3.2)$$

in the c.m.f.

$$p = p_\gamma^+ n_1 + \frac{M^2}{2p_\gamma^+} n_2, \quad p_\gamma^+ = \frac{M}{2}. \quad (3.3)$$

The distance between two particles according to the k_t algorithm [43] reads

$$d_{ij} = 2 \min(E_i^2, E_j^2) \frac{1 - \cos \theta_{ij}}{M^2} = \min\left(\frac{E_i}{E_j}, \frac{E_j}{E_i}\right) \frac{2p_i p_j}{M^2} = \min\left(\frac{p_i p}{p_j p}, \frac{p_j p}{p_i p}\right) \frac{2p_i p_j}{M^2}. \quad (3.4)$$

Here $E_{i,j}$, θ_{ij} are the particle's energies and the relative angle between them in c.m.f. Two particles belong to one jet if $d_{ij} < y_{cut}$. In our case $y_{cut} = 0.15$ [15].

One introduces the variables

$$\mathbf{x}_i = 2 \frac{E_i}{M} = \frac{2p p_i}{M^2} \leq 1, \quad (3.5)$$

which satisfy

$$\sum_{i=q,\bar{q},g} \mathbf{x}_i = 2, \quad \frac{2p_i p_j}{M^2} = 1 - \mathbf{x}_k = \bar{\mathbf{x}}_k, \quad d_{ij} = \min\left(\frac{\mathbf{x}_i}{\mathbf{x}_j}, \frac{\mathbf{x}_j}{\mathbf{x}_i}\right) (1 - \mathbf{x}_k). \quad (3.6)$$

In our variables

$$\frac{(x_{\bar{q}}\vec{p}_q - x_q\vec{p}_{\bar{q}})^2}{x_q x_{\bar{q}} M^2} = 1 - \mathbf{x}_q = \frac{(p - p_g)^2}{M^2} = \frac{(p_q + p_{\bar{q}})^2}{M^2} = \frac{2p_q p_{\bar{q}}}{M^2}, \quad (3.7)$$

$$\frac{(x_{\bar{q}}\vec{p}_g - z\vec{p}_{\bar{q}})^2}{z x_{\bar{q}} M^2} = 1 - \mathbf{x}_q, \quad \frac{(z\vec{p}_q - x_q\vec{p}_g)^2}{x_q z M^2} = 1 - \mathbf{x}_{\bar{q}}, \quad (3.8)$$

and using

$$\bar{\mathbf{x}}_q + \bar{\mathbf{x}}_{\bar{q}} + \bar{\mathbf{x}}_g = 1 \quad (3.9)$$

we have

$$M^2 = \frac{(x_{\bar{q}}\vec{p}_g - z\vec{p}_{\bar{q}})^2}{z x_{\bar{q}}} + \frac{(z\vec{p}_q - x_q\vec{p}_g)^2}{x_q z} + \frac{(x_{\bar{q}}\vec{p}_q - x_q\vec{p}_{\bar{q}})^2}{x_q x_{\bar{q}}}. \quad (3.10)$$

In the c.m.f. we also have

$$x_q + x_{\bar{q}} + z = 1, \quad \vec{p}_g + \vec{p}_q + \vec{p}_{\bar{q}} = 0. \quad (3.11)$$

3.2 Quark+gluon or antiquark+gluon in one jet

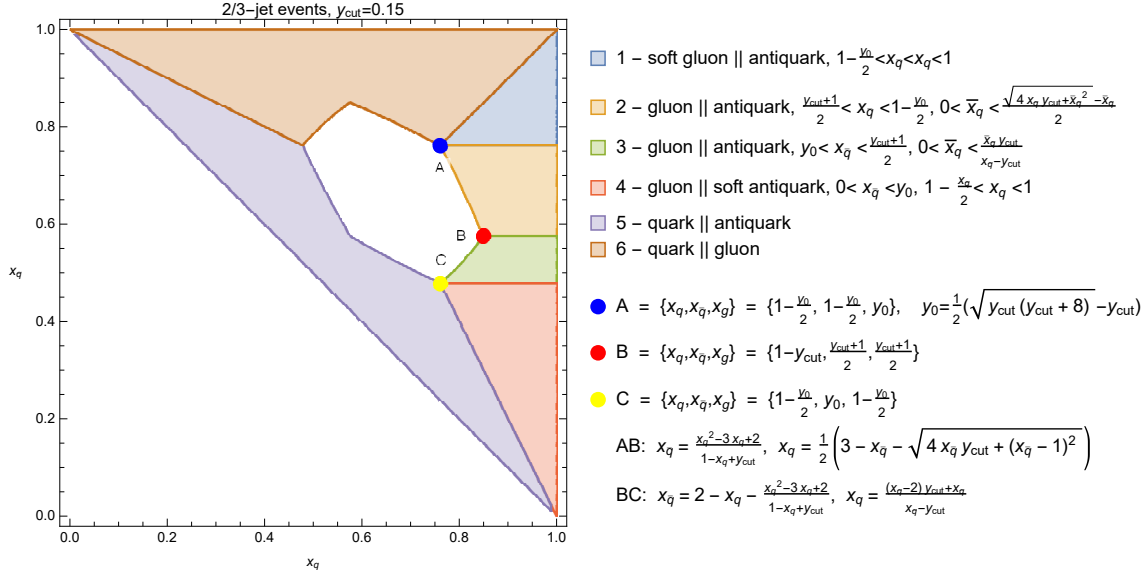


Figure 2: Dalitz plot for 2-3 jet separation in the exclusive k_t algorithm [43]. Regions 1–4 comprise the area of q - ($\bar{q}g$) dipole configuration, i.e. collinear antiquark and gluon. The dissection of the q – ($\bar{q}g$) dipole area covering the curved polygon with the vertices $(1, 1)$, A , B , C , $(1, 0)$ into regions is arbitrary. We found the tessellation depicted here convenient for integration.

The integral over the area covered by regions 1–4 in figure 2 gives the contribution of configurations where the antiquark and the gluon form one jet, jet i.e. when the gluon and the antiquark are almost collinear to each other. The other jet is then formed by the

quark. So we have

$$\vec{p}_j = \vec{p}_q, \quad x_j = x_q, \quad \vec{p}_{\bar{j}} = \vec{p}_{\bar{q}} + \vec{p}_g, \quad x_{\bar{j}} = x_{\bar{q}} + z, \quad \vec{\Delta}_q = \frac{x_{\bar{q}}\vec{p}_g - z\vec{p}_{\bar{q}}}{x_{\bar{q}} + z}, \quad (3.12)$$

$$\bar{\mathbf{x}}_q \sim \vec{\Delta}_q^2 \frac{x_j^2}{z(x_{\bar{j}} - z)} \frac{x_{\bar{j}}x_j}{\vec{p}_j^2} < f(\mathbf{x}_{\bar{q}}) \sim O(\sqrt{y_{cut}}), \quad \bar{\mathbf{x}}_{\bar{q}} = \frac{z}{x_{\bar{j}}} + O(\sqrt{y_{cut}}), \quad (3.13)$$

$$\bar{\mathbf{x}}_g = \frac{x_{\bar{q}}}{x_{\bar{j}}} + O(\sqrt{y_{cut}}), \quad M^2 = \frac{\vec{p}_j^2}{x_j x_{\bar{j}}} + O(\sqrt{y_{cut}}), \quad (3.14)$$

which follows from (3.7–3.10). Here f describes the inner border of Regions 1–4 along the curve connecting the points (1,1), A, B, C, (1,0).

The cross section for $q\bar{q}g$ production has a contribution $d\sigma_3$ with 2 dipole operators, a contribution $d\sigma_4$ with a dipole operator and a double dipole operator, and a contribution $d\sigma_5$ with 2 double dipole operators (see (6.5–6.8) in ref. [18]),

$$d\sigma_{(q\bar{q}g)} = d\sigma_3 + d\sigma_4 + d\sigma_5. \quad (3.15)$$

Here $d\sigma_3$ describes final state interaction and contains collinear and soft singularities while $d\sigma_4$ and $d\sigma_5$ are finite. Collinear singularities lie at $\mathbf{x}_q = 1$ and $\mathbf{x}_{\bar{q}} = 1$ and the soft one is in the corner $\mathbf{x}_q = \mathbf{x}_{\bar{q}} = 1$ in figure 2. In this paper we will work only with the singular part of $d\sigma_3$, where (see (7.8) of ref. [18])

$$d\sigma_3(x_q, \vec{p}_q)|_{\text{col}} = d\sigma(x_j, \vec{p}_j)|_{\text{Born}} \alpha_s \frac{\Gamma(1-\epsilon)}{(4\pi)^{1+\epsilon}} \frac{N_c^2 - 1}{2N_c} n_{\bar{j}}, \quad (3.16)$$

and the collinear factor $n_{\bar{j}}$ (see (7.9) in [18]) reads

$$n_{\bar{j}} = \frac{\mu^{-2\epsilon}}{\Gamma(1-\epsilon)\pi^{\frac{d}{2}}} \int_{\alpha}^{x_{\bar{j}}} \frac{dz}{z} \int_{\vec{\Delta}_q^2 < f\left(\frac{x_{\bar{j}}-z}{x_{\bar{j}}}\right) \frac{z(x_{\bar{j}}-z)}{x_j^2} \frac{\vec{p}_j^2}{x_{\bar{j}}x_j}} d^d \vec{\Delta}_q \frac{dz^2 + 4x_{\bar{j}}(x_{\bar{j}} - z)}{x_{\bar{j}}^2 \vec{\Delta}_q^2}. \quad (3.17)$$

Here we modified the integration area in $n_{\bar{j}}$ according to k_t jet algorithm whereas in ref. [18] we used cone algorithm. After integration we get

$$n_{\bar{j}} + n_j = 4 \left[\left(\ln \left(\frac{M^2}{\mu^2} \right) + \frac{1}{\epsilon} \right) \left(\ln \left(\frac{x_j x_{\bar{j}}}{\alpha^2} \right) - \frac{3}{2} \right) - \frac{1}{2} \ln^2 \left(\frac{x_j x_{\bar{j}}}{\alpha^2} \right) - \frac{1}{2} \ln^2 \left(\frac{x_j}{x_{\bar{j}}} \right) + w(y_{cut}) \right], \quad (3.18)$$

where

$$\begin{aligned}
w(y_{cut}) &= 2Li_2\left(-\frac{y_0}{2y_{cut}}\right) - Li_2\left(\frac{y_0^2}{4y_{cut}}\right) + 2Li_2\left(\frac{1-y_0}{1-y_{cut}}\right) + Li_2(y_{cut}) \\
&+ 2Li_2(1-y_0) - \ln^2\frac{y_0}{2} + \ln 2\left(2\ln(1-y_0) - \frac{5y_{cut}^2}{2} + 7y_{cut} - \frac{9}{2}\right) - \frac{2\pi^2}{3} \\
&+ \ln y_{cut}\left(\frac{y_0^2 + 2y_0 - 3y_{cut}^2 + 6y_{cut} - 3}{2} + 2\ln(1-y_0)\right) - \frac{y_0^2 + 2y_0 + 3}{2}\ln\frac{y_0}{2} \\
&+ \frac{y_{cut}^2 + 2y_{cut} - y_0(y_0 + 2)}{2}\ln(y_0 - y_{cut}) + \frac{3 - y_{cut}^2 - 2y_{cut}}{2}\ln(1 - y_{cut}) \\
&+ \frac{6y_{cut}^3 + y_{cut}^2(y_0 - 20) + 2y_{cut}(y_0^2 + 7y_0 + 16) + y_0(y_0^2 + 10y_0 + 14)}{4(2y_{cut} + y_0)} \\
&+ \ln^2\left(\frac{1-y_{cut}}{1-y_0}\right) + \frac{3}{2}(1-y_{cut})^2\ln(2y_{cut} + y_0) + \frac{1}{2}(y_0^2 + 2y_0 - 3)\ln(1-y_0). \quad (3.19)
\end{aligned}$$

Here

$$y_0 = \frac{\sqrt{y_{cut}(y_{cut} + 8)} - y_{cut}}{2}. \quad (3.20)$$

This result cancels soft and collinear singularities in the virtual part and we get instead of (7.24) in ref. [18]

$$S_R = n_{\bar{j}} + n_j + S_V + S_V^* \quad (3.21)$$

$$= 4 \left[-\frac{1}{2}\ln^2\left(\frac{x_j}{x_{\bar{j}}}\right) + w(y_{cut}) + 3 - \frac{\pi^2}{6} \right] \Big|_{y_{cut}=0.15} = 4 \left[-\frac{1}{2}\ln^2\left(\frac{x_j}{x_{\bar{j}}}\right) + 1.33 \right]. \quad (3.22)$$

In the small y_{cut} approximation

$$S_R = 4 \left[-\frac{1}{2}\ln^2\left(\frac{x_j}{x_{\bar{j}}}\right) - \frac{1}{2}\ln^2 y_{cut} - \frac{3}{2}\ln y_{cut} - \frac{7\pi^2}{12} + \frac{13}{2} - \ln 8 \right] + O(\sqrt{y_{cut}}). \quad (3.23)$$

The remaining contributions of $d\sigma_3$, $d\sigma_4$, and $d\sigma_5$ are suppressed in y_{cut} . Therefore the contribution of the soft and collinear gluons to the cross section after cancellation of divergencies with the virtual part reads

$$d\sigma_3(x_q, \vec{p}_q)|_{\text{col}} = d\sigma_0(x_j, \vec{p}_j) \frac{\alpha_s}{4\pi} \frac{N_c^2 - 1}{2N_c} S_R + O(\sqrt{y_{cut}}). \quad (3.24)$$

Nevertheless $O(\sqrt{y_{cut}})$ corrections for $y_{cut} = 0.15$ are substantial, e.g. the next (numerically largest) correction to S_R reads

$$S_R = 4 \left[-\frac{1}{2}\ln^2\left(\frac{x_j}{x_{\bar{j}}}\right) - 0.29 + 4\sqrt{2y_{cut}} \right] + O(y_{cut}), \quad 4\sqrt{2y_{cut}} \simeq 2.19. \quad (3.25)$$

It means that leading in y_{cut} contribution is numerically of the same order as $O(\sqrt{y_{cut}})$ corrections. But corrections of this order come from all other contributions to the cross section, i.e. the remaining part of $d\sigma_3$, $d\sigma_4$, and $d\sigma_5$ integrated over the whole 3-jet area (regions 1–6). Therefore the result for S_R alone can not be a good approximation. It has importance rather as a subtraction term for future full numerical calculation.

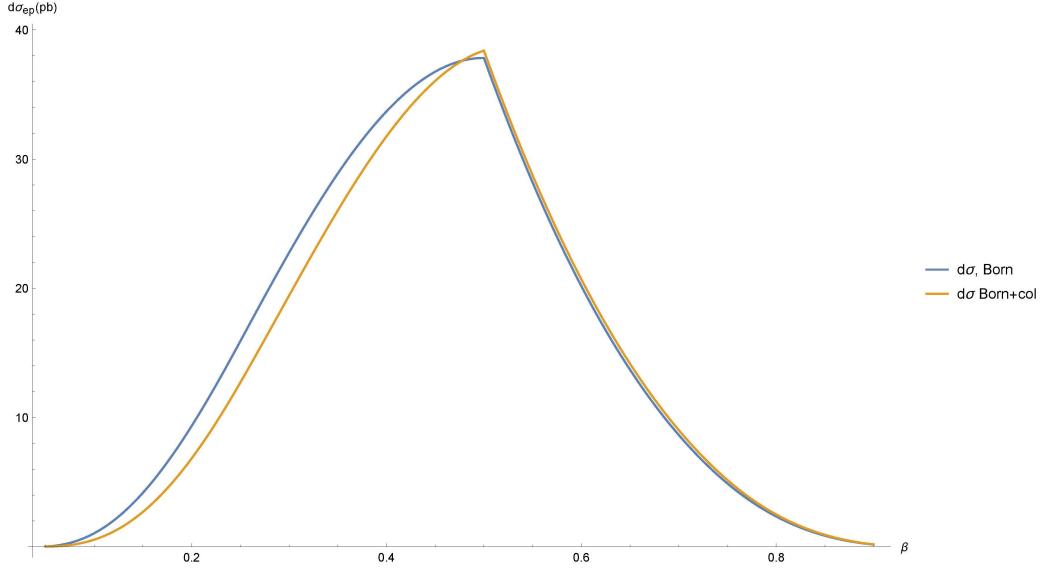


Figure 3: Born (2.94) and collinear correction (3.27) to e-p cross section.

Nevertheless using eq. (2.93),

$$\begin{aligned}
\left. \frac{d\sigma_3}{d\beta d\phi} \right|_{\text{col}} &= \frac{2\alpha^2 Q_q^2 N_c \sigma_0^2}{(2\pi)^4 B_G (\hbar c)^2} \frac{\alpha_s}{\pi} \frac{N_c^2 - 1}{2N_c} \\
&\times \int_{(1-x_{P_{\max}}\beta)}^{W_{\max}^2} \max\left(0.1s, \frac{Q_{\min}^2}{x_{P_{\max}}\beta}, \frac{Q_{\min}^2}{x_{P_{\max}}\beta}\right) \frac{dW^2}{s} \int_{\max(Q_{\min}^2, Q_{\min}^2 \frac{\beta}{1-x_{P_{\max}}\beta}, 0.1s-W^2)}^{\frac{x_{P_{\max}}\beta}{1-x_{P_{\max}}\beta} W^2} \frac{dQ^2}{y R_0^4 Q^6} \\
&\times \int_{x_{\min}}^{\bar{x}_{\min}} dx \left[\bar{y} \frac{(\bar{\beta} - \beta)^2 \beta^2}{x\bar{x}} + \frac{[(1-2x)^2 + 1]}{2} \frac{\bar{\beta}\beta^3}{(x\bar{x})^2} \left\{ \frac{1 + \bar{y}^2}{2} - \frac{2\bar{y}x\bar{x}}{1-2x\bar{x}} \cos(2\phi) \right\} \right] \\
&\times \left[w(y_{\text{cut}}) + 3 - \frac{\pi^2}{6} - \frac{1}{2} \ln^2\left(\frac{\bar{x}}{x}\right) \right]. \tag{3.26}
\end{aligned}$$

Then the x integral is doable analytically, see eq. (2.94)

$$\begin{aligned}
\left. \frac{d\sigma_{ep}}{d\beta d\phi} \right|_{\text{col}} &= \frac{\alpha_s}{\pi} \frac{N_c^2 - 1}{2N_c} \left[w(y_{\text{cut}}) + 3 - \frac{\pi^2}{6} \right] \left. \frac{d\sigma_{ep}}{d\beta d\phi} \right|_{\text{Born}} \\
&+ \frac{2\alpha^2 Q_q^2 N_c \sigma_0^2}{(2\pi)^4 B_G (\hbar c)^2} \int_{(1-x_{P_{\max}}\beta)}^{W_{\max}^2} \max\left(0.1s, \frac{Q_{\min}^2}{x_{P_{\max}}\beta}, \frac{Q_{\min}^2}{x_{P_{\max}}\beta}\right) \frac{dW^2}{s} \int_{\max(Q_{\min}^2, Q_{\min}^2 \frac{\beta}{1-x_{P_{\max}}\beta}, 0.1s-W^2)}^{\frac{x_{P_{\max}}\beta}{1-x_{P_{\max}}\beta} W^2} \frac{dQ^2}{y R_0^4 Q^6} \\
&\times \frac{\alpha_s}{\pi} \frac{N_c^2 - 1}{2N_c} \left[-\frac{1}{3} \ln^3\left(\frac{\bar{x}_{\min}}{x_{\min}}\right) (\bar{y}(\bar{\beta} - \beta)^2 \beta^2 - 2\bar{y}\bar{\beta}\beta^3 \cos(2\phi)) \right. \\
&\left. + \bar{\beta}\beta^3 \frac{1 + \bar{y}^2}{2} \frac{2(1-2x_{\min}\bar{x}_{\min}) \ln\left(\frac{\bar{x}_{\min}}{x_{\min}}\right) - (1-2x_{\min}) \left(\ln^2\left(\frac{\bar{x}_{\min}}{x_{\min}}\right) + 2 \right)}{x_{\min}\bar{x}_{\min}} \right]. \tag{3.27}
\end{aligned}$$

The result is given in figure 3. One may notice a sharp corner of the graph at $\beta = 0.5$. It is related to the change of the functional dependence on β in the limits of Q and W integrations of the cross section at $\beta = 0.5$, which is a consequence of the HERA cuts.

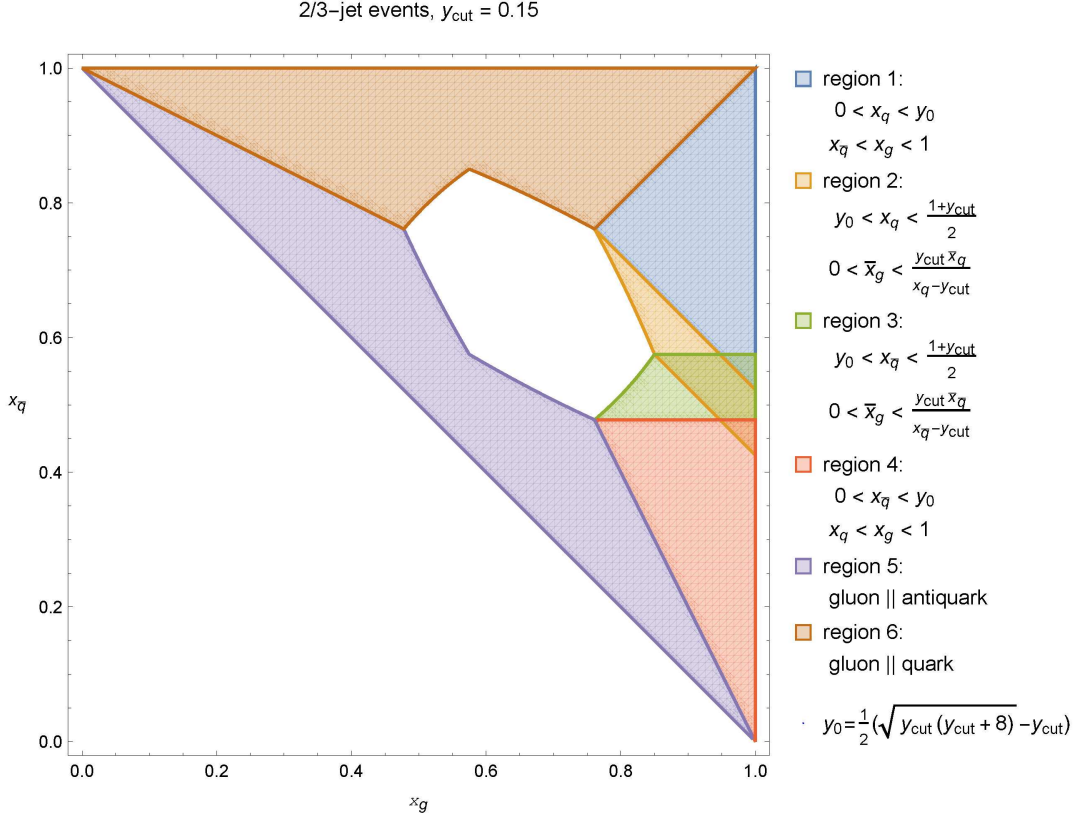


Figure 4: Dalitz plot for 2-3 jet separation in k_t exclusive algorithm [43]. Regions 1–4 comprise the area of gluon - ($q\bar{q}$) dipole configuration.

3.3 Quark+antiquark in one jet

The integral over the area covered by regions 1–4 in figure 4 is $\sim \sqrt{y_{\text{cut}}}$. These regions cover the configurations with a collinear quark-antiquark pair. However, this contribution may be enhanced in the large produced mass M limit thanks to the t -channel gluon in the impact factor. In this picture collinear $q\bar{q}$ configurations cover regions 1–4, where

$$\vec{p}_j = \vec{p}_g, \quad x_j = z, \quad \vec{p}_{\bar{j}} = \vec{p}_{\bar{q}} + \vec{p}_q, \quad x_{\bar{j}} = x_{\bar{q}} + x_q, \quad \vec{\Delta}_g = \frac{x_{\bar{q}}\vec{p}_q - x_q\vec{p}_{\bar{q}}}{x_{\bar{q}} + x_q}, \quad (3.28)$$

$$\bar{x}_g \sim \vec{\Delta}_g^2 \frac{x_j^2}{x_q(x_{\bar{j}} - x_q)} \frac{x_{\bar{j}}x_j}{\vec{p}_j^2} < f(\mathbf{x}_g) \sim O(\sqrt{y_{\text{cut}}}), \quad \bar{x}_{\bar{q}} = \frac{x_q}{x_{\bar{j}}} + O(\sqrt{y_{\text{cut}}}), \quad (3.29)$$

$$\bar{x}_q = \frac{x_{\bar{q}}}{x_{\bar{j}}} + O(\sqrt{y_{\text{cut}}}), \quad M^2 = \frac{\vec{p}_j^2}{x_j x_{\bar{j}}} + O(\sqrt{y_{\text{cut}}}), \quad (3.30)$$

which follows from (3.7–3.10).

The cross section for $q\bar{q}g$ production has a contribution $d\sigma_3$ with 2 dipole operators, a contribution $d\sigma_4$ with a dipole operator and a double dipole operator, and a contribution $d\sigma_5$ with 2 double dipole operators (see (6.5–6.8) in ref. [18]), see appendix C for proper normalization,

$$d\sigma_{(q\bar{q}g)} = d\sigma_3 + d\sigma_4 + d\sigma_5. \quad (3.31)$$

Since the photon in the initial state can appear with different polarizations, the various cross sections are labeled as

$$d\sigma_{JI} = \begin{pmatrix} d\sigma_{LL} & d\sigma_{LT} \\ d\sigma_{TL} & d\sigma_{TT} \end{pmatrix}, \quad d\sigma_{TL} = d\sigma_{LT}^*. \quad (3.32)$$

The dipole \times dipole contribution reads

$$\begin{aligned} d\sigma_{3JI} &= \alpha_s \frac{N_c^2 - 1}{N_c} \frac{1}{2(2\pi)^4} \frac{\alpha_{\text{em}} Q_q^2}{(2\pi)^4 N_c} \frac{(p_0^-)^2}{s^2 x_q x_{\bar{q}}} \varepsilon_{I\alpha} \varepsilon_{J\beta}^* dx_q dx_{\bar{q}} d^2 p_{q\perp} d^2 p_{\bar{q}\perp} \frac{dz d^2 p_{g\perp}}{z(2\pi)^2} \\ &\times \delta(1 - x_q - x_{\bar{q}} - z) \int d^2 p_{1\perp} d^2 p_{2\perp} d^2 p'_{1\perp} d^2 p'_{2\perp} \delta(p_{q1\perp} + p_{\bar{q}2\perp} + p_{g\perp}) \\ &\times \delta(p_{11'\perp} + p_{22'\perp}) \Phi_3^\alpha(p_{1\perp}, p_{2\perp}) \Phi_3^{\beta*}(p'_{1\perp}, p'_{2\perp}) \mathbf{F} \left(\frac{p_{12\perp}}{2} \right) \mathbf{F}^* \left(\frac{p_{1'2'\perp}}{2} \right). \end{aligned} \quad (3.33)$$

The dipole \times double dipole contribution reads

$$\begin{aligned} d\sigma_{4JI} &= \frac{1}{2(2\pi)^4} \alpha_s \frac{\alpha_{\text{em}} Q_q^2}{(2\pi)^4 N_c} \frac{(p_0^-)^2}{s^2 x_q x_{\bar{q}}} (\varepsilon_{I\alpha} \varepsilon_{J\beta}^*) dx_q dx_{\bar{q}} d^2 p_{q\perp} d^2 p_{\bar{q}\perp} \frac{dz d^2 p_{g\perp}}{z(2\pi)^2} \delta(1 - x_q - x_{\bar{q}} - z) \\ &\times \int d^2 p_{1\perp} d^2 p_{2\perp} d^2 p'_{1\perp} d^2 p'_{2\perp} \frac{d^2 p_{3\perp} d^2 p'_{3\perp}}{(2\pi)^2} \delta(p_{q1\perp} + p_{\bar{q}2\perp} + p_{g3\perp}) \delta(p_{11'\perp} + p_{22'\perp} + p_{33'\perp}) \\ &\times \left[\Phi_3^\alpha(p_{1\perp}, p_{2\perp}) \Phi_4^{\beta*}(p'_{1\perp}, p'_{2\perp}, p'_{3\perp}) \mathbf{F} \left(\frac{p_{12\perp}}{2} \right) \tilde{\mathbf{F}}^* \left(\frac{p_{1'2'\perp}}{2}, p'_{3\perp} \right) \delta(p_{3\perp}) \right. \\ &\left. + \Phi_4^\alpha(p_{1\perp}, p_{2\perp}, p_{3\perp}) \Phi_3^{\beta*} \left(\frac{p_{1'2'\perp}}{2} \right) \tilde{\mathbf{F}} \left(\frac{p_{12\perp}}{2}, p_{3\perp} \right) \mathbf{F}^* \left(\frac{p_{1'2'\perp}}{2} \right) \delta(p'_{3\perp}) \right]. \end{aligned} \quad (3.34)$$

The double dipole \times double dipole contribution to the 3 jet cross section reads

$$\begin{aligned} d\sigma_{5JI} &= \frac{1}{2(2\pi)^4} \alpha_s \frac{\alpha_{\text{em}} Q_q^2}{(2\pi)^4} \frac{(p_0^-)^2}{s^2 x_q x_{\bar{q}}} \frac{(\varepsilon_{I\alpha} \varepsilon_{J\beta}^*)}{N_c^2 - 1} dx_q dx_{\bar{q}} d^2 p_{q\perp} d^2 p_{\bar{q}\perp} \frac{dz d^2 p_{g\perp}}{z(2\pi)^2} \delta(1 - x_q - x_{\bar{q}} - z) \\ &\times \int d^2 p_{1\perp} d^2 p_{2\perp} d^2 p'_{1\perp} d^2 p'_{2\perp} \frac{d^2 p_{3\perp} d^2 p'_{3\perp}}{(2\pi)^4} \delta(p_{q1\perp} + p_{\bar{q}2\perp} + p_{g3\perp}) \delta(p_{11'\perp} + p_{22'\perp} + p_{33'\perp}) \\ &\times \Phi_4^\alpha(p_{1\perp}, p_{2\perp}, p_{3\perp}) \Phi_4^{\beta*}(p'_{1\perp}, p'_{2\perp}, p'_{3\perp}) \tilde{\mathbf{F}}_{p_{0\perp} p'_{0\perp}} \left(\frac{p_{12\perp}}{2}, p_{3\perp} \right) \tilde{\mathbf{F}}_{p_{0\perp} p'_{0\perp}}^* \left(\frac{p_{1'2'\perp}}{2}, p'_{3\perp} \right). \end{aligned} \quad (3.35)$$

Here the impact factors are given in ref. [18] and in Appendix B, whereas the hadronic matrix elements are given by eq. (5.3) of ref. [18]. Changing variables

$$\vec{p}_q, \vec{p}_{\bar{q}}, \vec{p}_g, x_q, z \rightarrow \vec{p} = \vec{p}_q + \vec{p}_{\bar{q}} + \vec{p}_g, \vec{p}_j, \vec{\Delta}_{\bar{q}}, x_q, x_j, \quad (3.36)$$

one gets

$$\begin{aligned} d\sigma_{3JI} &= \alpha_s \frac{N_c^2 - 1}{N_c^2} \frac{1}{2(2\pi)^4} \frac{\alpha_{\text{em}} Q_q^2}{(2\pi)^4} \frac{(p_0^-)^2}{s^2} (\varepsilon_{I\alpha} \varepsilon_{J\beta}^*) \frac{dx_q d\vec{p}_j d\vec{p} d\vec{\Delta}_{\bar{q}}}{x_q (1 - x_q - x_j) x_j (2\pi)^2} dx_j \\ &\times \int d^2 p_{1\perp} d^2 p_{2\perp} d^2 p'_{1\perp} d^2 p'_{2\perp} \delta(\vec{p}_1 + \vec{p}_2 - \vec{p}) \delta(p_{11'\perp} + p_{22'\perp}) \\ &\times \Phi_3^\alpha(p_{1\perp}, p_{2\perp}) \Phi_3^{\beta*}(p'_{1\perp}, p'_{2\perp}) \mathbf{F}_{p_{0\perp}, p_{0\perp} - p_{\perp}} \left(\frac{p_{12\perp}}{2} \right) \mathbf{F}_{p_{0\perp}, p_{0\perp} - p_{\perp}}^* \left(\frac{p_{1'2'\perp}}{2} \right), \end{aligned} \quad (3.37)$$

$$\begin{aligned}
d\sigma_{4JI} &= \alpha_s \frac{1}{2(2\pi)^4} \frac{\alpha_{\text{em}} Q_q^2 (p_0^-)^2 (\varepsilon_{I\alpha} \varepsilon_{J\beta}^*)}{(2\pi)^4 s^2 N_c} \frac{dx_q}{x_q(1-x_q-x_j)} \frac{dx_j}{x_j(2\pi)^2} d\vec{p}_j d\vec{p} d\vec{\Delta}_g \\
&\times \int d^2 p_{1\perp} d^2 p_{2\perp} d^2 p'_{1\perp} d^2 p'_{2\perp} \frac{d^2 p_{3\perp} d^2 p'_{3\perp}}{(2\pi)^2} \delta(\vec{p}_1 + \vec{p}_2 + \vec{p}_3 - \vec{p}) \delta(p_{11'\perp} + p_{22'\perp} + p_{33'\perp}) \\
&\times \left[\Phi_3^\alpha(p_{1\perp}, p_{2\perp}) \Phi_4^{\beta*}(p'_{1\perp}, p'_{2\perp}, p'_{3\perp}) \mathbf{F}_{p_{0\perp}, p_{0\perp} - p_\perp} \left(\frac{p_{12\perp}}{2} \right) \tilde{\mathbf{F}}_{p_{0\perp}, p_{0\perp} - p_\perp}^* \left(\frac{p_{1'2'\perp}}{2}, p'_{3\perp} \right) \delta(p_{3\perp}) \right. \\
&+ \left. \Phi_4^\alpha(p_{1\perp}, p_{2\perp}, p_{3\perp}) \Phi_3^{\beta*} \left(\frac{p_{1'2'\perp}}{2} \right) \tilde{\mathbf{F}}_{p_{0\perp}, p_{0\perp} - p_\perp} \left(\frac{p_{12\perp}}{2}, p_{3\perp} \right) \mathbf{F}_{p_{0\perp}, p_{0\perp} - p_\perp}^* \left(\frac{p_{1'2'\perp}}{2} \right) \delta(p'_{3\perp}) \right], \tag{3.38}
\end{aligned}$$

$$\begin{aligned}
d\sigma_{5JI} &= \alpha_s \frac{1}{2(2\pi)^4} \frac{\alpha_{\text{em}} Q_q^2 (p_0^-)^2 (\varepsilon_{I\alpha} \varepsilon_{J\beta}^*)}{(2\pi)^4 s^2 N_c^2 - 1} \frac{dx_q}{x_q(1-x_j-x_q)} \frac{dx_j}{x_j(2\pi)^2} d\vec{p}_j d\vec{p} d\vec{\Delta}_g \\
&\times \int d^2 p_{1\perp} d^2 p_{2\perp} d^2 p'_{1\perp} d^2 p'_{2\perp} \frac{d^2 p_{3\perp} d^2 p'_{3\perp}}{(2\pi)^4} \delta(\vec{p}_1 + \vec{p}_2 + \vec{p}_3 - \vec{p}) \delta(p_{11'\perp} + p_{22'\perp} + p_{33'\perp}) \\
&\times \Phi_4^\alpha(p_{1\perp}, p_{2\perp}, p_{3\perp}) \Phi_4^{\beta*}(p'_{1\perp}, p'_{2\perp}, p'_{3\perp}) \tilde{\mathbf{F}}_{p_{0\perp}, p_{0\perp} - p_\perp} \left(\frac{p_{12\perp}}{2}, p_{3\perp} \right) \tilde{\mathbf{F}}_{p_{0\perp}, p_{0\perp} - p_\perp}^* \left(\frac{p_{1'2'\perp}}{2}, p'_{3\perp} \right). \tag{3.39}
\end{aligned}$$

The hadronic matrix elements can be written as (see (5.2–5.8) in ref. [18])

$$\begin{aligned}
&2\pi \delta(p_{00'}) \tilde{\mathbf{F}}_{p_{0\perp} p'_{0\perp}} \left(\frac{p_{12\perp}}{2}, p_{3\perp} \right) \\
&= 2\pi \delta(p_{00'}) N_c (2\pi)^2 \left[\delta(\vec{p}_2) \mathbf{F}_{p_{0\perp} p'_{0\perp}} \left(\frac{p_{13\perp}}{2} \right) + \delta(\vec{p}_1) \mathbf{F}_{p_{0\perp} p'_{0\perp}} \left(\frac{p_{32\perp}}{2} \right) - \delta(\vec{p}_3) \mathbf{F}_{p_{0\perp} p'_{0\perp}} \left(\frac{p_{12\perp}}{2} \right) \right] \\
&+ \int d\vec{x} d\vec{y} e^{-i[(\frac{\vec{x}-\vec{y}}{2} \cdot \vec{p}_{12}) + (\frac{\vec{x}+\vec{y}}{2} \cdot \vec{p}_3)]} \\
&\times \langle P'(p'_0) | T \left[(tr(U_{\frac{x-y}{2}} U_{\frac{x+y}{2}}^\dagger) - N_c) (tr(U_{\frac{x+y}{2}} U_{\frac{y-x}{2}}^\dagger) - N_c) \right] | P(p_0) \rangle. \tag{3.40}
\end{aligned}$$

As a first approximation one may neglect the nonlinear term. Then we have

$$\begin{aligned}
&\tilde{\mathbf{F}}_{p_{0\perp} p'_{0\perp}} \left(\frac{p_{12\perp}}{2}, p_{3\perp} \right) \\
&\simeq N_c (2\pi)^2 \left[\delta(\vec{p}_2) \mathbf{F}_{p_{0\perp} p'_{0\perp}} \left(\frac{p_{13\perp}}{2} \right) + \delta(\vec{p}_1) \mathbf{F}_{p_{0\perp} p'_{0\perp}} \left(\frac{p_{32\perp}}{2} \right) - \delta(\vec{p}_3) \mathbf{F}_{p_{0\perp} p'_{0\perp}} \left(\frac{p_{12\perp}}{2} \right) \right] \tag{3.41}
\end{aligned}$$

$$= N_c (2\pi)^2 \left[\delta(\vec{p}_2) \mathbf{F} \left(\frac{p_{13\perp}}{2} \right) + \delta(\vec{p}_1) \mathbf{F} \left(\frac{p_{32\perp}}{2} \right) - \delta(\vec{p}_3) \mathbf{F} \left(\frac{p_{12\perp}}{2} \right) \right] e^{-\frac{B_G}{2} \vec{p}^2} \tag{3.42}$$

$$= -4\pi (2\pi)^2 N_c^2 \sigma_0 \left[\delta(\vec{p}_2) e^{-R_0^2 \vec{p}_1^2} \frac{\partial}{\partial p_1^2} + \delta(\vec{p}_1) e^{-R_0^2 \vec{p}_3^2} \frac{\partial}{\partial p_3^2} - \delta(\vec{p}_3) e^{-R_0^2 \vec{p}_2^2} \frac{\partial}{\partial p_2^2} \right] e^{-\frac{B_G}{2} \vec{p}^2}. \tag{3.43}$$

Intrinsically this assumes large N_c approximation so that we will neglect 1 in $N_c^2 - 1$. Integrating w.r.t. \vec{p} via

$$\int e^{-B_G \vec{p}^2} d\vec{p} = \frac{\pi}{B_G} \tag{3.44}$$

and substituting

$$dx_j d\vec{p}_j = dx_j d\phi \frac{d\vec{p}_j^2}{2} \rightarrow d\phi \frac{d\beta}{2\beta^2} Q^2 \int_{x_{\text{min}}}^{x_{\text{max}}} x_j x_{\bar{j}} dx_j, \tag{3.45}$$

one gets

$$\begin{aligned} \frac{d\sigma_{3JI}}{d\beta d\phi} &= \frac{1}{2} N_c^2 \sigma_0^2 \frac{\alpha_s \alpha_{\text{em}} Q_q^2 (p_0^-)^2 Q^2}{(2\pi)^7 B_G s^2 \beta^2} (\varepsilon_{I\alpha} \varepsilon_{J\beta}^*) \int_{x_{\min}}^{x_{\max}} x_{\bar{j}} dx_j \int_{\text{Regions 1-4}} \frac{dx_q d\vec{\Delta}_g}{x_q (1 - x_q - x_j)} \\ &\times \int d^2 p_{1\perp} d^2 p'_{1\perp} e^{-R_0^2 \vec{p}_1^2} \frac{\partial}{\partial p_1^2} \Phi_3^\alpha(p_{1\perp}, -p_{1\perp}) e^{-R_0^2 \vec{p}'_1^2} \frac{\partial}{\partial p_1'^2} \Phi_3^{\beta*}(p'_{1\perp}, -p'_{1\perp}), \end{aligned} \quad (3.46)$$

$$\begin{aligned} \frac{d\sigma_{4JI}}{d\beta d\phi} &= \frac{1}{2} N_c^2 \sigma_0^2 \frac{\alpha_s \alpha_{\text{em}} Q_q^2 (p_0^-)^2 Q^2}{(2\pi)^7 B_G s^2 \beta^2} (\varepsilon_{I\alpha} \varepsilon_{J\beta}^*) \int_{x_{\min}}^{x_{\max}} x_{\bar{j}} dx_j \int_{\text{Regions 1-4}} \frac{dx_q d\vec{\Delta}_g}{x_q (1 - x_q - x_j)} \\ &\times \int \left[\left(\delta(\vec{p}_2) e^{-R_0^2 \vec{p}_1^2} \frac{\partial}{\partial p_1^2} + \delta(\vec{p}_1) e^{-R_0^2 \vec{p}_3^2} \frac{\partial}{\partial p_3^2} - \delta(\vec{p}_3) e^{-R_0^2 \vec{p}_2^2} \frac{\partial}{\partial p_2^2} \right) \Phi_4^{\beta*}(p'_{1\perp}, p'_{2\perp}, p'_{3\perp}) \right. \\ &\times e^{-R_0^2 \vec{p}_1^2} \frac{\partial}{\partial p_1^2} \Phi_3^\alpha(p_{1\perp}, p_{2\perp}) \delta(p_{3\perp}) + e^{-R_0^2 \vec{p}'_1^2} \frac{\partial}{\partial p_1'^2} \Phi_3^{\beta*} \left(\frac{p_{1'2'\perp}}{2} \right) \delta(p'_{3\perp}) \\ &\times \left. \left(\delta(\vec{p}_2) e^{-R_0^2 \vec{p}_1^2} \frac{\partial}{\partial p_1^2} + \delta(\vec{p}_1) e^{-R_0^2 \vec{p}_3^2} \frac{\partial}{\partial p_3^2} - \delta(\vec{p}_3) e^{-R_0^2 \vec{p}_2^2} \frac{\partial}{\partial p_2^2} \right) \Phi_4^\alpha(p_{1\perp}, p_{2\perp}, p_{3\perp}) \right] \\ &\times d^2 p_{1\perp} d^2 p_{2\perp} d^2 p_{3\perp} d^2 p'_{1\perp} d^2 p'_{2\perp} d^2 p'_{3\perp} \delta(\vec{p}_1 + \vec{p}_2 + \vec{p}_3) \delta(p_{11'\perp} + p_{22'\perp} + p_{33'\perp}), \end{aligned} \quad (3.47)$$

$$\begin{aligned} \frac{d\sigma_{5JI}}{d\beta d\phi} &= \frac{1}{2} N_c^2 \sigma_0^2 \frac{\alpha_s \alpha_{\text{em}} Q_q^2 (p_0^-)^2 Q^2}{(2\pi)^7 B_G s^2 \beta^2} (\varepsilon_{I\alpha} \varepsilon_{J\beta}^*) \int_{x_{\min}}^{x_{\max}} x_{\bar{j}} dx_j \int_{\text{Regions 1-4}} \frac{dx_q d\vec{\Delta}_g}{x_q (1 - x_j - x_q)} \\ &\times \int \left[\delta(\vec{p}_2) e^{-R_0^2 \vec{p}_1^2} \frac{\partial}{\partial p_1^2} + \delta(\vec{p}_1) e^{-R_0^2 \vec{p}_3^2} \frac{\partial}{\partial p_3^2} - \delta(\vec{p}_3) e^{-R_0^2 \vec{p}_2^2} \frac{\partial}{\partial p_2^2} \right] \Phi_4^\alpha(p_{1\perp}, p_{2\perp}, p_{3\perp}) \\ &\times \left[\delta(\vec{p}'_2) e^{-R_0^2 \vec{p}'_1^2} \frac{\partial}{\partial p_1'^2} + \delta(\vec{p}'_1) e^{-R_0^2 \vec{p}'_3^2} \frac{\partial}{\partial p_3'^2} - \delta(\vec{p}'_3) e^{-R_0^2 \vec{p}'_2^2} \frac{\partial}{\partial p_2'^2} \right] \Phi_4^{\beta*}(p'_{1\perp}, p'_{2\perp}, p'_{3\perp})^* \\ &\times d^2 p_{1\perp} d^2 p_{2\perp} d^2 p_{3\perp} d^2 p'_{1\perp} d^2 p'_{2\perp} d^2 p'_{3\perp} \delta(\vec{p}_1 + \vec{p}_2 + \vec{p}_3) \delta(p_{11'\perp} + p_{22'\perp} + p_{33'\perp}). \end{aligned} \quad (3.48)$$

First, one has to integrate these expressions over the area covered by Regions 1–4 in the Dalitz plot (fig. 4). In terms of the plot variables \mathbf{x} the integral reads

$$\begin{aligned} \int_{\text{Regions 1-4}} d\mathbf{x}_g d\mathbf{x}_q &= \int_{\text{Regions 1-4}} d\mathbf{x}_g d\mathbf{x}_{\bar{q}} \\ &= \left[\int_{1-y_0}^1 d\bar{\mathbf{x}}_q \int_0^{\frac{x_q}{2}} d\bar{\mathbf{x}}_g + \int_{\frac{1-y_{\text{cut}}}{2}}^{1-y_0} d\bar{\mathbf{x}}_q \int_0^{\frac{y_{\text{cut}} \bar{\mathbf{x}}_q}{x_q - y_{\text{cut}}}} d\bar{\mathbf{x}}_g + (\mathbf{x}_q \leftrightarrow \mathbf{x}_{\bar{q}}) \right] \\ &\quad - \int_{\frac{1-y_{\text{cut}}}{2}}^{\frac{1+y_{\text{cut}}}{2}} d\bar{\mathbf{x}}_q \int_0^{\frac{1+y_{\text{cut}}}{2} - \bar{\mathbf{x}}_q} d\bar{\mathbf{x}}_g. \end{aligned} \quad (3.49)$$

Since the impact factor is symmetric w.r.t. $q \leftrightarrow \bar{q}$ interchange, one can rewrite the latter expression as

$$\begin{aligned} \int_{\text{Regions 1-4}} d\mathbf{x}_g d\mathbf{x}_q &= 2 \int_{1-y_0}^1 d\bar{\mathbf{x}}_q \int_0^{\frac{x_q}{2}} d\bar{\mathbf{x}}_g + 2 \int_{\frac{1-y_{\text{cut}}}{2}}^{1-y_0} d\bar{\mathbf{x}}_q \int_0^{\frac{y_{\text{cut}} \bar{\mathbf{x}}_q}{x_q - y_{\text{cut}}}} d\bar{\mathbf{x}}_g \\ &\quad - \int_{\frac{1-y_{\text{cut}}}{2}}^{\frac{1+y_{\text{cut}}}{2}} d\bar{\mathbf{x}}_q \int_0^{\frac{1+y_{\text{cut}}}{2} - \bar{\mathbf{x}}_q} d\bar{\mathbf{x}}_g. \end{aligned} \quad (3.50)$$

The impact factors are not singular as $\Delta_g \equiv |\vec{\Delta}_g| \rightarrow 0$ and $\vec{\Delta}_g^2 \sim \bar{\mathbf{x}}_g$. Therefore to get the leading in $\sqrt{y_{cut}}$ contribution, one can put $\Delta_g = 0$ in them and integrate w.r.t. Δ_g

$$\begin{aligned}
\int_{\text{Regions 1-4}} dx_q d\vec{\Delta}_g &= \frac{\vec{p}_j^2}{x_{\bar{j}} x_j} \pi x_{\bar{j}} \int_{\text{Regions 1-4}} d\mathbf{x}_g d\mathbf{x}_{\bar{q}} \frac{x_q (x_{\bar{j}} - x_q)}{x_{\bar{j}}^2} \\
&= 2\pi \frac{\vec{p}_j^2}{x_{\bar{j}} x_j} \int_{x_{\bar{j}}(1-y_0)}^{x_{\bar{j}}} dx_q \frac{1}{2} \frac{x_{\bar{j}} - x_q}{x_{\bar{j}}} \frac{x_q (x_{\bar{j}} - x_q)}{x_{\bar{j}}^2} \\
&+ 2\pi \frac{\vec{p}_j^2}{x_{\bar{j}} x_j} \int_{x_{\bar{j}} \frac{1-y_{cut}}{2}}^{x_{\bar{j}}(1-y_0)} dx_q y_{cut} \frac{1 - \frac{x_{\bar{j}} - x_q}{x_{\bar{j}}}}{\frac{x_{\bar{j}} - x_q}{x_{\bar{j}}} - y_{cut}} \frac{x_q (x_{\bar{j}} - x_q)}{x_{\bar{j}}^2} + O(y_{cut}). \quad (3.51)
\end{aligned}$$

Next, we will work in the small Q_s approximation as we did for the LO impact factor (see eqs. (2.88–2.92)). It means that after integrating out delta-functions and calculating derivatives in eqs. (3.46–3.48), one takes the angular integrals of the remaining t -channel momenta ($\vec{p}_1^{(l)}, \vec{p}_2^{(l)}$, or $\vec{p}_3^{(l)}$) and neglects their absolute values everywhere except in the exponents. Then the exponential integrals are calculated straightforwardly giving $\int_0^{+\infty} dp^2 e^{-R_0^2 p^2} = \frac{1}{R_0^2}$. As a result one has the following cross sections

$$\frac{d\sigma_{LL}}{d\beta d\phi} = \frac{1}{2} N_c^2 \sigma_0^2 \frac{\alpha_s \alpha_{em} Q_q^2 \sqrt{2y_{cut}}}{(2\pi)^4 B_G R_0^4 Q^4} a + O(y_{cut}), \quad (3.52)$$

$$\frac{d\sigma_{TT}^{ij}}{d\beta d\phi} = \frac{1}{2} N_c^2 \sigma_0^2 \frac{\alpha_s \alpha_{em} Q_q^2 \sqrt{2y_{cut}}}{(2\pi)^4 B_G R_0^4 Q^4} (c g_{\perp}^{ij} + b e^{(x)i} e^{(x)j}) + O(y_{cut}), \quad (3.53)$$

$$a = a_3 + a_4 + a_5, \quad b = b_3 + b_4 + b_5, \quad c = c_3 + c_4 + c_5. \quad (3.54)$$

Here $a_i, b_i, c_i, i = 3, 4, 5$ are the contributions coming from eqs. (3.46–3.48) correspondingly.

We demonstrate this procedure on the example of the longitudinal photon contribution to σ_5 . The impact factor for longitudinal photon \times longitudinal photon was calculated in ref. [18] (B.1). It reads

$$\begin{aligned}
&\frac{(p_0^-)^2}{s^2} \varepsilon_{L\alpha} \Phi_4^\alpha(p_{1\perp}, p_{2\perp}, p_{3\perp}) \varepsilon_{L\beta}^* \Phi_4^\beta(p'_{1\perp}, p'_{2\perp}, p'_{3\perp})^* \\
&= 4Q^2 \frac{(x_q^2 + (x_q + z)^2) x_{\bar{q}}^2}{x_q x_{\bar{q}} z^2} \vec{V}_q(p_1, p_3) \vec{V}_q(p'_1, p'_3) \\
&- 4Q^2 \frac{(x_{\bar{q}} + z) x_q + (x_q + z) x_{\bar{q}}}{z^2} \vec{V}_q(p_1, p_3) \vec{V}_{\bar{q}}(p'_2, p'_3) + (x_q, p_1, p'_1, V_q \leftrightarrow x_{\bar{q}}, p_2, p'_2, V_{\bar{q}}), \quad (3.55)
\end{aligned}$$

where

$$\vec{V}_q(p_1, p_3) = \frac{x_q \vec{p}_{q3} - z \vec{p}_{q1}}{(x_q + z) \left(\frac{(\vec{p}_{q3} + \vec{p}_{q1})^2}{x_{\bar{q}}} + \frac{p_{q3}^2}{z} + \frac{p_{q1}^2}{x_q} + Q^2 \right) \left(\frac{(\vec{p}_{q3} + \vec{p}_{q1})^2}{x_{\bar{q}}(x_q + z)} + Q^2 \right)}. \quad (3.56)$$

As was outlined above, using small Q_s and small y_{cut} approximations, one can take t -

channel integrals

$$\begin{aligned}
& \int \left[\delta(\vec{p}_2) e^{-R_0^2 \vec{p}_1^2} \frac{\partial}{\partial p_1^2} + \delta(\vec{p}_1) e^{-R_0^2 \vec{p}_3^2} \frac{\partial}{\partial p_3^2} - \delta(\vec{p}_3) e^{-R_0^2 \vec{p}_2^2} \frac{\partial}{\partial p_2^2} \right] \\
& \times \delta(\vec{p}_1 + \vec{p}_2 + \vec{p}_3) \vec{V}_q(p_1, p_3) d^2 p_{1\perp} d^2 p_{2\perp} d^2 p_{3\perp} \\
& = \int \left[\delta(\vec{p}_2) e^{-R_0^2 \vec{p}_1^2} \frac{\partial}{\partial p_1^2} + \delta(\vec{p}_1) e^{-R_0^2 \vec{p}_3^2} \frac{\partial}{\partial p_3^2} - \delta(\vec{p}_3) e^{-R_0^2 \vec{p}_2^2} \frac{\partial}{\partial p_2^2} \right] \\
& \times \delta(\vec{p}_1 + \vec{p}_2 + \vec{p}_3) \vec{V}_q(p_2, p_3) d^2 p_{1\perp} d^2 p_{2\perp} d^2 p_{3\perp} \Big|_{x_q \rightarrow x_{\bar{q}} = 1 - x_j - x_q} \\
& \simeq \frac{\pi \beta^3 \bar{p}_j}{R_0^2 Q^6} \left(\frac{(\beta + 1)x_q + 2x_j(x_{\bar{j}} - x_q)}{(x_j(x_{\bar{j}} - x_q) + \beta x_q)^2} - \frac{4}{x_{\bar{j}} x_j} \right). \tag{3.57}
\end{aligned}$$

Then one integrates over regions 1–4 via eq. (3.51) and w.r.t. x_j according to eq. (3.45). Keeping only the leading contribution y_{cut} , one gets

$$a_5 = 8\beta^2 \bar{\beta}^2 \ln \frac{\bar{x}_{\min}}{x_{\min}}. \tag{3.58}$$

The product of the transverse photon \times transverse photon impact factor $\Phi_4^i(p_{1\perp}, p_{2\perp}, p_{3\perp}) \Phi_4^j(p'_{1\perp}, p'_{2\perp}, p'_{3\perp})^*$ was calculated in ref. [18], see eq. (B.16). The integration in this case is similar to the previous case, albeit with more cumbersome expressions. Therefore we do not present the intermediate results giving only the final answer

$$b_5 = 2\bar{\beta}^2 (4\beta^2 - 1) \ln \frac{\bar{x}_{\min}}{x_{\min}}, \tag{3.59}$$

$$c_5 = \frac{\bar{\beta}}{4\beta} (8\bar{\beta}\beta^3 - 2\beta - 1) \frac{1 - 2x_{\min}}{x_{\min} \bar{x}_{\min}} + \bar{\beta} (4\bar{\beta}\beta^2 - 1) \ln \frac{\bar{x}_{\min}}{x_{\min}}. \tag{3.60}$$

The longitudinal photon \times longitudinal photon impact factor $\Phi_3^+(p_{1\perp}, p_{2\perp}) \Phi_3^+(p'_{1\perp}, p'_{2\perp})^*$ was calculated in eqs. (B.2–4) and the transverse one in eqs. (B.17–19) in ref. [18]. They lead to

$$a_3 = \beta^2 \left((4\beta(2\beta - 3) + 7) \ln \frac{\bar{x}_{\min}}{x_{\min}} - (1 - 2x_{\min}) \right), \tag{3.61}$$

$$b_3 = \bar{\beta} \left((\bar{\beta} + 4\beta^2 - 8\beta^3) \ln \frac{\bar{x}_{\min}}{x_{\min}} + (1 + \beta)(1 - 2x_{\min}) \right), \tag{3.62}$$

$$c_3 = \frac{\bar{\beta}}{4\beta} \left(\beta^2 \frac{4\beta - 8\beta^2 - 3}{x_{\min} \bar{x}_{\min}} - 1 \right) (1 - 2x_{\min}) + \frac{\bar{\beta}}{2} (4\beta^2 + 1) (1 - 2\beta) \ln \frac{\bar{x}_{\min}}{x_{\min}}. \tag{3.63}$$

The remaining cross section $d\sigma_{4JI}$ contains $\Phi_4(p_{1\perp}, p_{2\perp}, p_{3\perp}) \Phi_3(p'_{1\perp}, p'_{2\perp})^*$. We present these convolutions in the Appendix B. Integrating them according to the guidelines discussed above we get

$$a_4 = 4\beta^2 \bar{\beta} (3 - 4\beta) \ln \frac{\bar{x}_{\min}}{x_{\min}}, \tag{3.64}$$

$$b_4 = 2\bar{\beta} (6\beta^2 - 8\beta^3 - 1) \ln \frac{\bar{x}_{\min}}{x_{\min}}, \tag{3.65}$$

$$c_4 = \frac{\bar{\beta}\beta}{2} (1 + 6\beta - 8\beta^2) \frac{1 - 2x_{\min}}{x_{\min} \bar{x}_{\min}} + \frac{\bar{\beta}}{2\beta} (2\beta^2(6\beta - 8\beta^2 - 1) + 1) \ln \frac{\bar{x}_{\min}}{x_{\min}}. \tag{3.66}$$

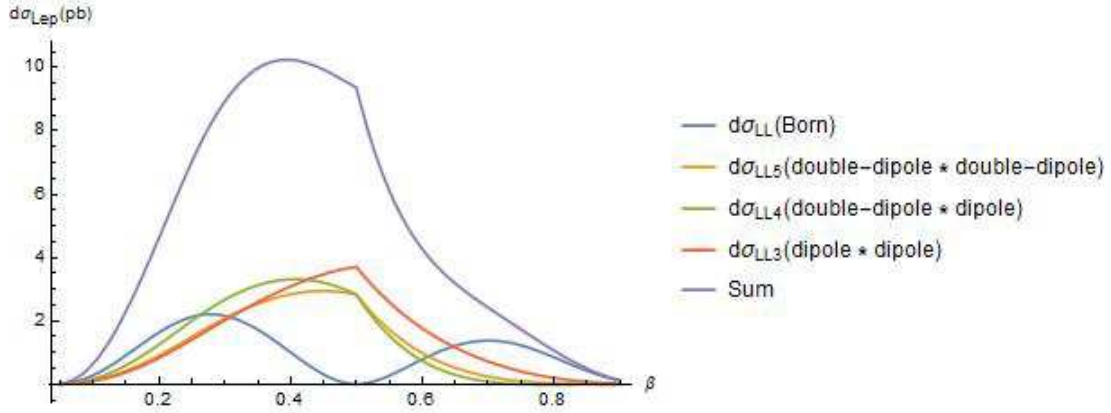


Figure 5: $ep \rightarrow ep + 2jets$ cross-section in the case of a longitudinal photon. Born and gluon dipole contributions.

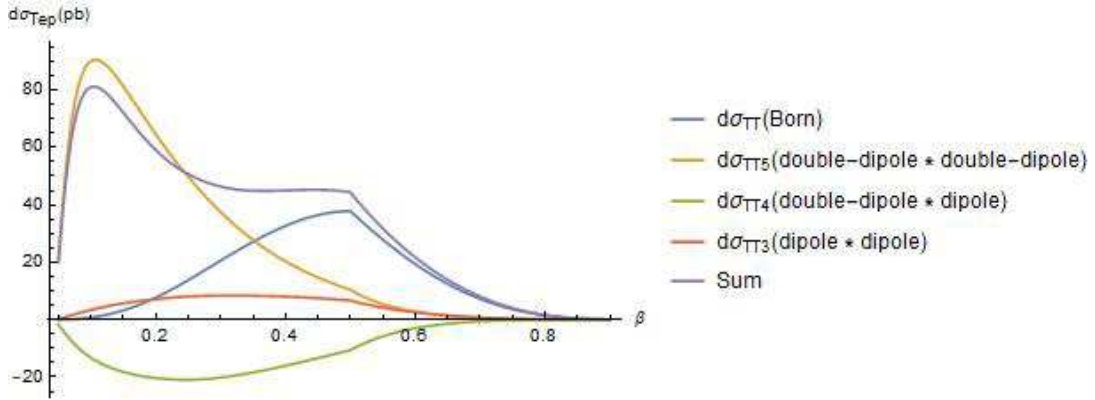


Figure 6: $ep \rightarrow ep + 2jets$ cross-section in the case of a transverse photon. Born and gluon dipole contributions.

Now one can recall the relation between the γ^*P and eP cross sections (2.21) and write, see eqs. (3.52–3.54),

$$\begin{aligned} \left. \frac{d\sigma_{ep}}{d\beta d\phi} \right|_{\text{gluon dipole}} &= \frac{\alpha^2 \alpha_s Q_q^2}{B_G (\hbar c)^2} \frac{\sqrt{2y_{cut}}}{(2\pi)^5} N_c^2 \sigma_0^2 \int_{(1-x_{Pmax}\beta) \max(0.1s, \frac{Q_{min}^2}{x_{Pmax}\beta}, \frac{Q_{min}^2}{x_{Pmax}\beta})}^{W_{max}^2} \frac{dW^2}{s} \\ &\times \int_{\max(Q_{min}^2, Q_{min}^2 \frac{\beta}{\beta}, 0.1s-W^2)}^{\frac{x_{Pmax}\beta}{1-x_{Pmax}\beta} W^2} \frac{dQ^2}{y R_0^4 Q^6} \left[2\bar{y}a + \frac{1+\bar{y}^2}{2}(b-2c) + \bar{y}b \cos(2\phi) \right]. \end{aligned} \quad (3.67)$$

To get the distribution in β one has to integrate this equation w.r.t. ϕ from 0 to π because jets are treated as identical. The results are in figures 5, 6, 7. As one can see, the interference term $d\sigma_{4T}$ is negative, which significantly diminishes the leading power asymptotics of $d\sigma_{5T}$. In addition, the large N_c approximation decreases $d\sigma_{5T}$ for $\sim 10\%$ since we expand $\frac{N_c^4}{N_c^2-1} \simeq N_c^2$. On the other hand the rapidity cut (2.75–2.76) dependence is very low.

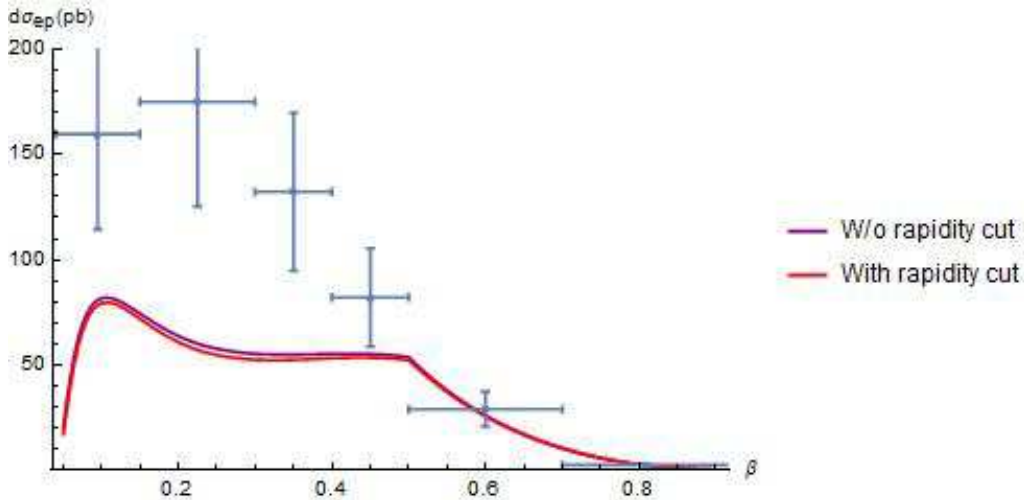


Figure 7: Born and total gluon dipole contributions to cross section vs experimental data from [15]. Rapidity cut is defined in (2.75–2.76).

4. Conclusion

This paper discussed the exclusive diffractive dijet electroproduction with HERA selection cuts [15]. We started from the analytic formulas from ref. [18] for fully differential Born cross section and its real correction with dipole \times dipole and double dipole \times double dipole configurations. In addition, in appendix B we calculated the remaining interference real production impact factor with dipole \times double dipole configuration. We used the GBW parametrization for the dipole matrix element between the proton states and the large N_c approximation for the double dipole matrix elements. We constructed the differential $ep \rightarrow ep + 2jets$ cross section in $\beta = \frac{Q^2}{Q^2 + M_{2jets}^2}$ and in the angle ϕ between the leptonic and hadronic planes with HERA acceptance. We argued that HERA selection rules [15] suppress the aligned jet contribution indicative of saturation to the Born cross section. These cuts allowed us to neglect the t -channel momentum in the Born impact factor and integrate the γp cross section analytically. The result is in eq. (2.94).

Next, we cancelled the singularities from soft and collinear gluons between real and virtual corrections in the collinear approximation by integrating the singular contributions over the $q - (\bar{q}g)$ and $\bar{q} - (qg)$ areas in the Dalitz plot of fig. 2 within the k_t jet algorithm. As the Born cross section, the resulting correction was analytically integrated in the small Q_s approximation in ref. (3.27). It gives $\sim 10\%$ of the Born result.

Finally, we integrated all real corrections in the small Q_s and small y_{cut} approximations over the the $g - (q\bar{q})$ area in the Dalitz plot of fig. 4 within the k_t jet algorithm. This configuration gives the dominant contribution in the small β region thanks to Regge enhancement because of the diagram with t -channel gluon at large $s = M_{2jet}^2$. The results for this gluon dipole configuration are in refs. (3.52–3.54) and refs. (3.58–3.67). Results for Born and gluon dipole in the small Q_s approximation together give about $\frac{1}{2}$ of the measured cross section.

We noted that firstly, the small Q_s approximation works for Born, collinearly enhanced radiative corrections to $q\bar{q}$ dipole configuration, and generic gluon dipole configuration since the HERA cuts Q , $M_{2jets} > 5$ GeV and $p_{\perp \min} > 2$ GeV effectively restrict jets with very small longitudinal momentum fraction x . It means that the typical hard scale in the impact factor is of order of M_{2jets}^2 , Q^2 , $M_{2jets}^2 x$, $Q^2 x$, $p_{\perp \min}^2$ and multiplication with x here can not make it smaller than Q_s^2 . So we can expand the impact factor in Q_s . However for Born, the region $x < Q_s^2 / \max(Q^2, M_{2jets}^2)$ is the aligned jet region indicative of saturation.

Secondly, this approximation fails for other corrections to $q\bar{q}$ dipole configuration since Q_s may be the largest scale in the impact factor in them. It also fails for gluon dipole configuration when the $q\bar{q}$ pair forming one of the jets is in the aligned jet configuration itself since the longitudinal momentum fraction of q or \bar{q} may be the small parameter making the impact factor scales smaller than Q_s .

Thirdly, we nevertheless calculated the gluon dipole contribution in the small Q_s approximation neglecting that it may be incorrect in the aforementioned corners of the phase space. Therefore comparison of our answer to the full numerical result will show how important these contributions are. This is left for future studies.

Finally, we noted that the corrections in y_{cut} may be significant since the real expansion parameter is $\sqrt{y_{cut}} = \sqrt{0.15} \simeq 0.39$. Therefore the $O(\sqrt{y_{cut}})$ corrections to $q\bar{q}$ dipole configuration which we did not calculate may give sizable corrections. However we expect these corrections as well as the nonsingular virtual corrections to be peaked at moderate β as the Born term.

Acknowledgments

We thank G. Gach, K. Golec-Biernat, D. Yu. Ivanov, C. Marquet, S. Munier, B. Schenke for many useful discussions. A. V. G. acknowledges support of RFBR grant 19-02-00690. This work was supported in part by the Ministry of Education and Science of the Russian Federation. He thanks the GDR QCD for support. The work of R. B. is supported by the U.S. Department of Energy, Office of Nuclear Physics, under Contracts No. DE-SC0012704 and by an LDRD grant from Brookhaven Science Associates. L. S. is supported by the grant 2017/26/M/ST2/01074 of the National Science Center in Poland. He thanks the French LABEX P2IO, the French GDR QCD and the LPT for support. Part of the calculations were done on the supercomputer of Novosibirsk State University.

A. Scaling of the aligned versus symmetric jet contributions

As was discussed in the text, $F_T^{D(3)}$ is a higher twist correction when compared to ref. (2.102) as it has an extra power of $Q^2 R_0^2 \gg 1$ in its denominator. The origin of this suppression lies in the fact that the dominant contribution to the transverse cross section comes from the aligned jet configuration, i.e. the region of $x \lesssim \frac{1}{\max(Q^2, M^2) R_0^2} \ll 1$. One can see it from

eq. (2.87):

$$A = \frac{\sigma_0}{|\vec{p}_{q\bar{q}}|} \int_0^{+\infty} dp^2 e^{-R_0^2 \vec{p}^2} \frac{\partial}{\partial p^2} \frac{x\bar{x}Q^2 + p^2 - (\frac{\vec{p}_{q\bar{q}}}{2})^2}{\sqrt{(x\bar{x}Q^2 + p^2 + (\frac{\vec{p}_{q\bar{q}}}{2})^2)^2 - 4p^2(\frac{\vec{p}_{q\bar{q}}}{2})^2}} \quad (\text{A.1})$$

$$\sim \int_0^1 da \frac{\sigma_0 M Q^2 R_0^2 x^{\frac{3}{2}}}{[(x(M^2 + Q^2)R_0^2 + a)^2 - 4M^2 R_0^2 a x]^{\frac{3}{2}}} \quad (\text{A.2})$$

$$= \frac{\sigma_0}{m\sqrt{x}} \left(\frac{M^2 - Q^2}{M^2 + Q^2} + \frac{1 + xR_0^2(Q^2 - M^2)}{\sqrt{1 + 2xR_0^2(Q^2 - M^2) + x^2R_0^4(Q^2 + M^2)^2}} \right), \quad (\text{A.3})$$

where we approximated $e^{-R_0^2 \vec{p}^2} \simeq \theta(R_0^{-2} - \vec{p}^2)$. Then we get the known behavior of eq. (2.102)

$$x_P F_T^{D(3)}|_{Q^2 \gg M^2} \sim \frac{Q^4}{\beta B_G} \int_0^{\frac{1}{Q^2 R_0^2}} A^2 x dx \sim \frac{Q^4}{\beta^2 B_G} \frac{M^2 \sigma_0^2}{Q^6 R_0^2} = \frac{\bar{\beta} \sigma_0^2}{B_G R_0^2}, \quad (\text{A.4})$$

$$x_P F_T^{D(3)}|_{M^2 \gg Q^2} \sim \frac{Q^4}{\beta B_G} \int_0^{\frac{1}{M^2 R_0^2}} A^2 x dx \sim \frac{Q^4}{\beta B_G} \frac{\sigma_0^2}{M^4 R_0^2} = \frac{\beta \sigma_0^2}{B_G R_0^2}. \quad (\text{A.5})$$

It is easier to observe in the coordinate space (following ref. [42]), where eqs. (2.79–2.80) can be cast into

$$\frac{d\sigma_{T,L}^{\gamma P}}{dM^2} = \frac{3\alpha}{32\pi^2 B_G} \sum e_f^2 \int dx \left\{ \frac{(x^2 + \bar{x}^2)x^2 \bar{x}^2 Q^2 (\int r dr J_1(\sqrt{x\bar{x}}Mr) K_1(\sqrt{x\bar{x}}Qr) \hat{\sigma}(r))^2}{4x^3 \bar{x}^3 Q^2 (\int r dr J_0(\sqrt{x\bar{x}}Mr) K_0(\sqrt{x\bar{x}}Qr) \hat{\sigma}(r))^2} \right\}, \quad (\text{A.6})$$

$$x_P F_{T,L}^{D(3)} = \frac{Q^4}{4\pi^2 \alpha \beta} \frac{d\sigma_{T,L}^{\gamma P}}{dM^2}, \quad \hat{\sigma}(r) = \sigma_0 (1 - e^{-\frac{r^2}{4R_0^2}}). \quad (\text{A.7})$$

In the large β region $Q^2 R_0^2 \gg 1$, $Q^2 \gg \frac{1}{R_0^2} \gg M^2$ the longitudinal cross section reads

$$\begin{aligned} \int r dr J_0(\sqrt{x\bar{x}}Mr) K_0(\sqrt{x\bar{x}}Qr) \hat{\sigma}(r) &\sim \left(\int_0^{\left(\frac{2}{Q}\right)^2} + \int_{\frac{2}{Q}}^{\frac{1}{x\bar{x}Q^2}} \right) dr^2 \hat{\sigma}(r) \\ &\sim \int_0^{\left(\frac{2}{Q}\right)^2} \frac{r^2}{R_0^2} dr^2 + \theta\left(x > \frac{1}{Q^2 R_0^2}\right) \int_{\left(\frac{2}{Q}\right)^2}^{\frac{1}{x\bar{x}Q^2}} \frac{r^2}{R_0^2} dr^2 \\ &+ \theta\left(x < \frac{1}{Q^2 R_0^2}\right) \int_{\left(\frac{2}{Q}\right)^2}^{R_0^2} \frac{r^2}{R_0^2} dr^2 + \theta\left(x < \frac{1}{Q^2 R_0^2}\right) \int_{R_0^2}^{\frac{1}{x\bar{x}Q^2}} dr^2 \end{aligned} \quad (\text{A.8})$$

$$\sim \frac{1}{Q^4 R_0^2} + \theta\left(x > \frac{1}{Q^2 R_0^2}\right) \frac{1}{x^2 Q^4 R_0^2} + \theta\left(x < \frac{1}{Q^2 R_0^2}\right) \frac{1}{x Q^2}, \quad (\text{A.9})$$

where neglecting logarithms

$$J_0(\sqrt{x\bar{x}}Mr) \sim 1, \quad K_0(\sqrt{x\bar{x}}Qr) \sim \theta(1 - \sqrt{x\bar{x}}Qr). \quad (\text{A.10})$$

$$\begin{aligned}
\frac{d\sigma_L^{\gamma p}}{dM^2} &\sim \int_0^1 (x\bar{x})^3 dx \left[\left(\frac{1}{Q^4 R_0^2} \right)^2 + \theta \left(x > \frac{1}{Q^2 R_0^2} \right) \left(\frac{1}{x Q^4 R_0^2} \right)^2 \right. \\
&\quad + \theta \left(x > \frac{1}{Q^2 R_0^2} \right) \left(\frac{1}{x^2 Q^4 R_0^2} \right)^2 + \theta \left(x < \frac{1}{Q^2 R_0^2} \right) \frac{1}{x Q^2} \frac{1}{Q^4 R_0^2} \\
&\quad \left. + \theta \left(x < \frac{1}{Q^2 R_0^2} \right) \left(\frac{1}{x Q^2} \right)^2 \right], \tag{A.11}
\end{aligned}$$

$$\frac{d\sigma_L^{\gamma p}}{dM^2} \sim \frac{1}{Q^8 R_0^4} + \frac{1}{Q^8 R_0^4} \ln \frac{1}{Q^2 R_0^2} + \left(\frac{1}{Q^2 R_0^2} \right)^3 \frac{1}{Q^6 R_0^2} + \frac{1}{Q^8 R_0^4}. \tag{A.12}$$

So at $\beta \sim 1$, $x_P F_L^{D(3)} \sim \frac{1}{Q^4 R_0^4}$ and this dominant contribution comes from the whole region in x .

The transverse cross section in the large β region $Q^2 R_0^2 \gg 1$, $Q^2 \gg \frac{1}{R_0^2} \gg M^2$ reads

$$\begin{aligned}
\int r dr J_1(\sqrt{x\bar{x}}Mr) K_1(\sqrt{x\bar{x}}Qr) \hat{\sigma}(r) &\sim \frac{\sqrt{x\bar{x}}Mr}{\sqrt{x\bar{x}}Qr} \left(\int_0^{\frac{2}{Q}} + \int_{\frac{2}{Q}}^{\frac{1}{x\bar{x}Q^2}} \right) dr^2 \hat{\sigma}(r) \\
&\sim \frac{M}{Q} \left(\int_0^{\left(\frac{2}{Q}\right)^2} \frac{r^2}{R_0^2} dr^2 + \theta \left(x > \frac{1}{Q^2 R_0^2} \right) \int_{\left(\frac{2}{Q}\right)^2}^{\frac{1}{x\bar{x}Q^2}} \frac{r^2}{R_0^2} dr^2 \right. \\
&\quad \left. + \theta \left(x < \frac{1}{Q^2 R_0^2} \right) \left(\int_{\frac{1}{Q^2}}^{R_0^2} \frac{r^2}{R_0^2} + \int_{R_0^2}^{\frac{1}{x\bar{x}Q^2}} \right) dr^2 \right) \\
&\sim \frac{M}{Q} \left[\frac{1}{Q^4 R_0^2} + \theta \left(x > \frac{1}{Q^2 R_0^2} \right) \frac{1}{x^2 Q^4 R_0^2} + \theta \left(x < \frac{1}{Q^2 R_0^2} \right) \frac{1}{x Q^2} \right], \tag{A.13}
\end{aligned}$$

where

$$J_1(\sqrt{x\bar{x}}Mr) \sim \sqrt{x\bar{x}}Mr, \quad K_1(\sqrt{x\bar{x}}Qr) \sim \frac{\theta(1 - \sqrt{x\bar{x}}Qr)}{\sqrt{x\bar{x}}Qr}. \tag{A.14}$$

$$\begin{aligned}
\frac{d\sigma_T^{\gamma p}}{dM^2} &\sim \frac{M^2}{Q^2} \int_0^1 (x\bar{x})^2 dx \left[\left(\frac{1}{Q^4 R_0^2} \right)^2 + \theta \left(x > \frac{1}{Q^2 R_0^2} \right) \frac{1}{x^2} \left(\frac{1}{Q^4 R_0^2} \right)^2 \right. \\
&\quad + \theta \left(x > \frac{1}{Q^2 R_0^2} \right) \left(\frac{1}{x^2 Q^4 R_0^2} \right)^2 + \theta \left(x < \frac{1}{Q^2 R_0^2} \right) \left(\frac{1}{x Q^2} \right) \frac{1}{Q^4 R_0^2} \\
&\quad \left. + \theta \left(x < \frac{1}{Q^2 R_0^2} \right) \left(\frac{1}{x Q^2} \right)^2 \right], \tag{A.15}
\end{aligned}$$

$$\frac{d\sigma_T^{\gamma p}}{dM^2} \sim \frac{M^2}{Q^2} \left[\frac{1}{Q^8 R_0^4} + \frac{Q^2 R_0^2}{Q^8 R_0^4} + \left(\frac{1}{Q^2 R_0^2} \right)^2 \frac{1}{Q^6 R_0^2} + \frac{1}{Q^4} \frac{1}{Q^2 R_0^2} \right]. \tag{A.16}$$

So at $\beta \sim 1$, $x_P F_T^{D(3)} \sim \frac{1}{Q^4 R_0^2}$ and this dominant contribution comes from $x < \frac{1}{Q^2 R_0^2}$, i.e. aligned jets.

In the small β region $Q^2 R_0^2 \gg 1$, $M^2 R_0^2 \gg 1$, $M^2 \gg Q^2 \gg \frac{1}{R_0^2}$ for the longitudinal cross section we have

$$\begin{aligned}
\int r dr J_0(\sqrt{x\bar{x}}Mr) K_0(\sqrt{x\bar{x}}Qr) \hat{\sigma}(r) &\sim \left(\int_0^{\frac{2}{M}} + \int_{\frac{2}{M}}^{\frac{1}{x\bar{x}M^2}} \right) dr^2 \hat{\sigma}(r) \\
&\sim \int_0^{\left(\frac{2}{M}\right)^2} \frac{r^2}{R_0^2} dr^2 + \theta\left(x > \frac{1}{M^2 R_0^2}\right) \int_{\left(\frac{2}{M}\right)^2}^{\frac{1}{xM^2}} \frac{r^2}{R_0^2} dr^2 + \theta\left(x < \frac{1}{M^2 R_0^2}\right) \left(\int_{\frac{1}{M^2}}^{R_0^2} \frac{r^2}{R_0^2} + \int_{R_0^2}^{\frac{1}{xM^2}} \right) dr^2 \\
&\sim \frac{1}{M^4 R_0^2} + \theta\left(x > \frac{1}{M^2 R_0^2}\right) \frac{1}{x^2 M^4 R_0^2} + \theta\left(x < \frac{1}{M^2 R_0^2}\right) \frac{1}{xM^2}, \tag{A.17}
\end{aligned}$$

where again neglecting logarithms

$$J_0(\sqrt{x\bar{x}}Mr) \sim \theta(1 - \sqrt{x\bar{x}}Mr), \quad K_0(\sqrt{x\bar{x}}Qr) \sim 1. \tag{A.18}$$

$$\begin{aligned}
\frac{d\sigma_L^{\gamma P}}{dM^2} &\sim \int_0^1 (x\bar{x})^3 dx \left[\left(\frac{1}{M^4 R_0^2} \right)^2 + \theta\left(x > \frac{1}{M^2 R_0^2}\right) \left(\frac{1}{xM^4 R_0^2} \right)^2 \right. \\
&+ \theta\left(x > \frac{1}{M^2 R_0^2}\right) \left(\frac{1}{x^2 M^4 R_0^2} \right)^2 + \theta\left(x < \frac{1}{M^2 R_0^2}\right) \left(\frac{1}{xM^2} \right) \frac{1}{M^4 R_0^2} \\
&\left. + \theta\left(x < \frac{1}{M^2 R_0^2}\right) \left(\frac{1}{xM^2} \right)^2 \right], \tag{A.19}
\end{aligned}$$

i.e.

$$\frac{d\sigma_L^{\gamma P}}{dM^2} \sim \frac{1}{M^8 R_0^4} + \frac{1}{m^8 R_0^4} \ln \frac{1}{M^2 R_0^2} + \left(\frac{1}{M^2 R_0^2} \right)^3 \frac{1}{M^6 R_0^2} + \frac{1}{M^8 R_0^4}. \tag{A.20}$$

Therefore

$$x_P F_L^{D(3)} \sim \frac{\beta^3}{R_0^4} \tag{A.21}$$

and this contribution comes from the whole region in x . In the small β region $Q^2 R_0^2 \gg 1$, $M^2 R_0^2 \gg 1$, $M^2 \gg Q^2 \gg \frac{1}{R_0^2}$ for the transverse cross section we have

$$\begin{aligned}
\int r dr J_1(\sqrt{x\bar{x}}Mr) K_1(\sqrt{x\bar{x}}Qr) \hat{\sigma}(r) &\sim \frac{\sqrt{x\bar{x}}Mr}{\sqrt{x\bar{x}}Qr} \left(\int_0^{\frac{2}{M}} + \int_{\frac{2}{M}}^{\frac{1}{x\bar{x}M^2}} \right) dr^2 \hat{\sigma}(r) \\
&\sim \frac{M}{Q} \left(\int_0^{\left(\frac{2}{M}\right)^2} \frac{r^2}{R_0^2} dr^2 + \theta\left(x > \frac{1}{M^2 R_0^2}\right) \int_{\left(\frac{2}{M}\right)^2}^{\frac{1}{xM^2}} \frac{r^2}{R_0^2} dr^2 + \theta\left(x < \frac{1}{M^2 R_0^2}\right) \int_{R_0^2}^{\frac{1}{xM^2}} dr^2 \right) \\
&\sim \frac{M}{Q} \left[\frac{1}{M^4 R_0^2} + \theta\left(x > \frac{1}{M^2 R_0^2}\right) \frac{1}{x^2 M^4 R_0^2} + \theta\left(x < \frac{1}{M^2 R_0^2}\right) \frac{1}{xM^2} \right], \tag{A.22}
\end{aligned}$$

where

$$J_1(\sqrt{x\bar{x}}Mr) \sim \sqrt{x\bar{x}}Mr \theta(1 - \sqrt{x\bar{x}}Mr), \quad K_1(\sqrt{x\bar{x}}Qr) \sim \frac{1}{\sqrt{x\bar{x}}Qr}. \tag{A.23}$$

$$\begin{aligned}
\frac{d\sigma_T^{\gamma p}}{dM^2} &\sim \frac{M^2}{Q^2} \int_0^1 (x\bar{x})^2 dx \left[\left(\frac{1}{M^4 R_0^2} \right)^2 + \theta\left(x > \frac{1}{M^2 R_0^2}\right) \frac{1}{x^2} \left(\frac{1}{M^4 R_0^2} \right)^2 \right. \\
&+ \theta\left(x > \frac{1}{M^2 R_0^2}\right) \left(\frac{1}{x^2 M^4 R_0^2} \right)^2 + \theta\left(x < \frac{1}{M^2 R_0^2}\right) \left(\frac{1}{x M^2} \right) \frac{1}{M^4 R_0^2} \\
&\left. + \theta\left(x < \frac{1}{M^2 R_0^2}\right) \left(\frac{1}{x M^2} \right)^2 \right], \tag{A.24}
\end{aligned}$$

i.e.

$$\frac{d\sigma_T^{\gamma p}}{dM^2} \sim \frac{M^2}{Q^2} \left[\frac{1}{M^8 R_0^4} + \frac{M^2 R_0^2}{M^8 R_0^4} + \left(\frac{1}{M^2 R_0^2} \right)^2 \frac{1}{M^6 R_0^2} + \frac{1}{M^4} \frac{1}{M^2 R_0^2} \right]. \tag{A.25}$$

$$x_P F_T^{D(3)} = \frac{Q^4}{4\pi^2 \alpha \beta} \frac{d\sigma_{T,L}^{\gamma p \rightarrow X p'}}{dM^2} \sim \frac{1}{\beta} \frac{1}{M^4 R_0^2} \sim \frac{\beta}{R_0^2}. \tag{A.26}$$

Again this dominant contribution comes from $x < \frac{1}{M^2 R_0^2}$, i.e. aligned jets.

B. Dipole-double dipole interference terms

Unfortunately [18] does not contain expressions for interference terms necessary for calculation of $d\sigma_4$. We present them here. The calculation is straightforward and goes along the lines described in [18]. In the notation of that paper the result reads

$$\Phi_4^+(p_{1\perp}, p_{2\perp}, p_{3\perp}) \Phi_3^+(p'_{1\perp}, p'_{2\perp})^* = \Phi_4^+(p_{1\perp}, p_{2\perp}, p_{3\perp}) \Phi_4^+(p'_{1\perp}, p'_{2\perp}, 0)^* + C^{++}, \tag{B.1}$$

$$\begin{aligned}
C^{++} &= \frac{8p_\gamma^{+4}}{z(x_q + z) \left(\frac{\vec{p}_{q2}^2}{x_{\bar{q}}(x_q + z)} + Q^2 \right) \left(\frac{\vec{p}_{q1}^2}{x_q} + \frac{\vec{p}_{q2}^2}{x_{\bar{q}}} + \frac{p_{g3}^2}{z} + Q^2 \right)} \\
&\times \left\{ \frac{(4x_q x_{\bar{q}} + z(2 - dz)) (\vec{p}_g - \frac{z}{x_{\bar{q}}} \vec{p}_{\bar{q}}) (x_q \vec{p}_{g3} - z \vec{p}_{q1})}{(\vec{p}_g - \frac{z \vec{p}_{\bar{q}}}{x_{\bar{q}}})^2 \left(\frac{\vec{p}_{q1'}^2}{x_q(x_q + z)} + Q^2 \right)} \right. \\
&\left. - \frac{x_{\bar{q}} (dz^2 + 4x_q(x_q + z)) (p_g - \frac{z}{x_q} \vec{p}_q) (p_{g3} - \frac{z}{x_q} \vec{p}_{q1})}{(\vec{p}_g - \frac{z \vec{p}_q}{x_q})^2 \left(\frac{\vec{p}_{q2'}^2}{x_{\bar{q}}(x_q + z)} + Q^2 \right)} \right\} \\
&+ (p_q \leftrightarrow p_{\bar{q}}, p_1^{(\prime)} \leftrightarrow p_2^{(\prime)}, x_q \leftrightarrow x_{\bar{q}}). \tag{B.2}
\end{aligned}$$

$$\Phi_4^i(p_{1\perp}, p_{2\perp}, p_{3\perp}) \Phi_3^k(p'_{1\perp}, p'_{2\perp})^* = \Phi_4^i(p_{1\perp}, p_{2\perp}, p_{3\perp}) \Phi_4^k(p'_{1\perp}, p'_{2\perp}, 0)^* + C^{ik}, \tag{B.3}$$

$$\begin{aligned}
C^{ik} = & \frac{2p_\gamma^{+2}}{\vec{\Delta}_q^2 \left(Q^2 + \frac{\vec{p}_{g3}^2}{z} + \frac{\vec{p}_{q1}^2}{x_q} + \frac{\vec{p}_{\bar{q}2}^2}{x_{\bar{q}}} \right) \left(Q^2 + \frac{\vec{p}_{\bar{q}2'}^2}{(z+x_q)x_{\bar{q}}} \right)} \\
& \times \left[\frac{((d-2)z - 2x_q) x_q}{(z+x_q)^3} \left(g_\perp^{ik} (\vec{p}_{\bar{q}2'} \vec{\Delta}_q) + p_{\bar{q}2'\perp}^i \Delta_{q\perp}^k + p_{\bar{q}2'\perp}^k \Delta_{q\perp}^i (1 - 2x_{\bar{q}}) \right) \right. \\
& + \frac{x_q \left(((d-4)z - 2x_q) \left(g_\perp^{ik} (\vec{p}_{\bar{q}2'} \vec{\Delta}_q) + p_{\bar{q}2'\perp}^i \Delta_{q\perp}^k \right) + p_{\bar{q}2'\perp}^k \Delta_{q\perp}^i (dz + 2x_q) (1 - 2x_{\bar{q}}) \right)}{(z+x_q)^2 (z+x_{\bar{q}})} \\
& - \frac{1}{z(z+x_q)^2 x_{\bar{q}} (z+x_{\bar{q}})^2 \left(Q^2 + \frac{\vec{p}_{q1}^2}{x_q(z+x_{\bar{q}})} \right)} \left\{ z((d-4)z + 2) \right. \\
& \times \left[p_{q1\perp}^i \left((\vec{p}_{\bar{q}2'} \vec{\Delta}_q) P_\perp^k - (\vec{P} \vec{p}_{\bar{q}2'}) \Delta_{q\perp}^k \right) (2x_q - 1) - (\vec{P} \vec{p}_{\bar{q}2'}) \left(g_\perp^{ik} (\vec{p}_{q1} \vec{\Delta}_q) + p_{q1\perp}^k \Delta_{q\perp}^i \right) \right. \\
& - P_\perp^k \left((\vec{p}_{q1} \vec{\Delta}_q) p_{\bar{q}2'\perp}^i - (\vec{p}_{q1} \vec{p}_{\bar{q}2'}) \Delta_{q\perp}^i \right) \left. \right] + 4x_q z (1 - 2x_q) p_{q1\perp}^i \left((\vec{p}_{\bar{q}2'} \vec{\Delta}_q) P_\perp^k - (\vec{P} \vec{p}_{\bar{q}2'}) \Delta_{q\perp}^k \right) \\
& + z(1 - 2x_{\bar{q}}) (dz + 4x_q - 2) p_{\bar{q}2'\perp}^k \left((\vec{p}_{q1} \vec{\Delta}_q) P_\perp^i - (\vec{P} \vec{p}_{q1}) \Delta_{q\perp}^i \right) - z((d-4)z - 2) \\
& \times \left[\left(g_\perp^{ik} (\vec{P} \vec{p}_{q1}) + P_\perp^i p_{q1\perp}^k \right) (\vec{p}_{\bar{q}2'} \vec{\Delta}_q) + \left((\vec{P} \vec{p}_{q1}) p_{\bar{q}2'\perp}^i - (\vec{p}_{q1} \vec{p}_{\bar{q}2'}) P_\perp^i \right) \Delta_{q\perp}^k \right] \\
& + (\vec{P} \vec{\Delta}_q) p_{q1\perp}^i p_{\bar{q}2'\perp}^k (1 - 2x_q) (1 - 2x_{\bar{q}}) (z(dz - 2) - 4x_q x_{\bar{q}}) \\
& - (\vec{P} \vec{\Delta}_q) \left(g_\perp^{ik} (\vec{p}_{q1} \vec{p}_{\bar{q}2'}) + p_{q1\perp}^k p_{\bar{q}2'\perp}^i \right) (z(2 - (d-4)z) + 4x_q x_{\bar{q}}) \left. \right\} \\
& - \frac{1}{z(z+x_q)^4 \left(Q^2 + \frac{\vec{p}_{\bar{q}2}^2}{(z+x_q)x_{\bar{q}}} \right) x_{\bar{q}}} \left\{ z(dz + 4x_{\bar{q}} - 4) \left[(1 - 2x_{\bar{q}}) \right. \right. \\
& \times \left(p_{\bar{q}2'\perp}^k \left((\vec{p}_{\bar{q}2} \vec{\Delta}_q) W_\perp^i - (\vec{W} \vec{p}_{\bar{q}2}) \Delta_{q\perp}^i \right) + p_{\bar{q}2\perp}^i \left((\vec{W} \vec{p}_{\bar{q}2'}) \Delta_{q\perp}^k - (\vec{p}_{\bar{q}2'} \vec{\Delta}_q) W_\perp^k \right) \right. \\
& + W_\perp^k \left((\vec{p}_{\bar{q}2} \vec{\Delta}_q) p_{\bar{q}2'\perp}^i - (\vec{p}_{\bar{q}2} \vec{p}_{\bar{q}2'}) \Delta_{q\perp}^i \right) + \left. \left((\vec{p}_{\bar{q}2} \vec{p}_{\bar{q}2'}) W_\perp^i - (\vec{W} \vec{p}_{\bar{q}2}) p_{\bar{q}2'\perp}^i \right) \Delta_{q\perp}^k \right. \\
& + g_\perp^{ik} \left((\vec{W} \vec{p}_{\bar{q}2'}) (\vec{p}_{\bar{q}2} \vec{\Delta}_q) - (\vec{W} \vec{p}_{\bar{q}2}) (\vec{p}_{\bar{q}2'} \vec{\Delta}_q) \right) + p_{\bar{q}2\perp}^k \left((\vec{W} \vec{p}_{\bar{q}2'}) \Delta_{q\perp}^i - (\vec{p}_{\bar{q}2'} \vec{\Delta}_q) W_\perp^i \right) \left. \right] \\
& + (\vec{W} \vec{\Delta}_q) \left(p_{\bar{q}2\perp}^i p_{\bar{q}2'\perp}^k (1 - 2x_{\bar{q}})^2 - g_\perp^{ik} (\vec{p}_{\bar{q}2} \vec{p}_{\bar{q}2'}) - p_{\bar{q}2\perp}^k p_{\bar{q}2'\perp}^i \right) (dz^2 - 4x_q (x_{\bar{q}} - 1)) \left. \right\} \\
& + (p_q \leftrightarrow p_{\bar{q}}, p_1^{(i)} \leftrightarrow p_2^{(i)}, x_q \leftrightarrow x_{\bar{q}}), \tag{B.4}
\end{aligned}$$

where

$$W_\perp^i = x_q p_{g3\perp}^i - z p_{q1\perp}^i, \quad P_\perp^i = x_{\bar{q}} p_{g3\perp}^i - z p_{\bar{q}2\perp}^i. \tag{B.5}$$

C. Normalization

In this appendix we discuss the overall normalization of the cross section and the relation of our matrix elements F defined in (5.2–8) of ref. [18] to the GBW dipole cross section.

The density matrix for the LO cross section in our frame (5.21-23) was obtained in ref. [18]. To get the proper normalization we have to multiply all cross sections in ref. [18] by $\frac{1}{2(2\pi)^4}$. Indeed, the factor $\frac{1}{2}$ comes from the normalization of A_3 in eq. (5.11) of ref. [18].

The in and out proton states are normalized there to have

$$\frac{1}{\sqrt{2p_0^-}\sqrt{2p_0'^-}} \simeq \frac{1}{\sqrt{4E_0}\sqrt{4E_0'}} = \frac{1}{2} \frac{1}{\sqrt{2E_0}\sqrt{2E_0'}}. \quad (\text{C.1})$$

Since the S-matrix does not depend on state normalization, A_3 is two times bigger than the standard amplitude normalized to $\frac{1}{\sqrt{2E_0}\sqrt{2E_0'}}$. As a result, the cross section should have an extra $\frac{1}{4}$ to compensate for it, i.e. in (5.1) of ref. [18] we should have had

$$d\sigma = \frac{1}{4} \frac{1}{2s} (2\pi)^4 \delta^{(4)}(p_\gamma + p_0 - p_q - p_{\bar{q}} - p_0') |A_3|^2 d\rho_3. \quad (\text{C.2})$$

The same correction must be done in eq. (6.1) of ref. [18].

The 2π power must be corrected in eq. (5.11) of ref. [18] in the overall factor

$$\frac{1}{(2\pi)^{D-4}} \rightarrow \frac{1}{(2\pi)^{D-2}}. \quad (\text{C.3})$$

Indeed, the amplitude A_3 is exactly the matrix element (3.1) of ref. [18] after removing $(2\pi)^4 \delta^{(4)}(p_\gamma + p_0 - p_q - p_{\bar{q}} - p_0')$. In this matrix element transverse and $(-)$ delta functions appear together with $(2\pi)^2$ and 2π as eqs. (5.7–8) and eqs. (5.2–3) of ref. [18] correspondingly. Only the $(+)$ delta function is without 2π in eq. (3.1). Therefore we must have an extra 2π in the denominator in A_3 in addition to $\frac{1}{(2\pi)^{D-3}}$ from eq. (3.1) of ref. [18]. This gives us the aforementioned substitution. The same misprint was done in eq. (6.4) of ref. [18]. After these corrections we get eqs. (2.22–2.25).

Next, we have to substitute a model for the hadronic matrix elements \mathbf{F} . We will use the Golec-Biernat - Wüsthoff (GBW) [45] parametrization, which was formulated in the coordinate space. To get the proper normalization we Fourier transform eq. (2.23) and compare it with Eq. (4.48) in ref. [42]. Using

$$\frac{1}{\vec{l}^2 + a^2} = \int d^2r \frac{K_0(ar)}{2\pi} e^{-i\vec{l}\vec{r}}, \quad \mathbf{F}(\vec{k}) = \int d\vec{r} e^{-i\vec{k}\vec{r}} F(\vec{r}), \quad (\text{C.4})$$

we have

$$\left. \frac{d\sigma_{0LL}}{dx d\vec{p}_q d\vec{p}_{\bar{q}}} \right|_{t=0} = \frac{1}{2(2\pi)^4} \frac{4\alpha Q_q^2}{N_c} x^2 \bar{x}^2 Q^2 \left| \int d^2r \frac{K_0(\sqrt{x\bar{x}}Qr)}{2\pi} e^{i\frac{pq\bar{q}\perp}{2}\vec{r}} F(\vec{r}) \right|^2 \quad (\text{C.5})$$

and

$$\left. \frac{d\sigma_{0LL}}{dt} \right|_{t=0} = \frac{1}{2(2\pi)^4} \frac{4\alpha Q_q^2}{N_c} \pi \int dx Q^2 x^2 \bar{x}^2 \int d^2r K_0(\sqrt{x\bar{x}}Qr)^2 F(\vec{r})^2. \quad (\text{C.6})$$

Comparing it with eq. (4.48) in ref. [42], the GBW parametrization of the forward dipole matrix element in our normalization reads

$$\begin{aligned} F_{p_{0\perp} p_{0\perp}}(z_\perp) &= \left. \frac{\langle P'(p_0') | T(\text{Tr}(U_{\frac{z_\perp}{2}} U_{-\frac{z_\perp}{2}}^\dagger) - N_c) | P(p_0) \rangle}{2\pi \delta(p_{00'})} \right|_{p_0 \rightarrow p_0'} \\ &= F(z_\perp) = N_c \sigma_0 (1 - e^{-\frac{z_\perp^2}{4R_0^2}}). \end{aligned} \quad (\text{C.7})$$

One can check the consistency of this normalization by deriving the inclusive γ^*p cross section with the same matrix elements. Using propagators in the shockwave background (2.19–20) from ref. [18], one gets for the $\gamma^*p \rightarrow \gamma^*p$ amplitude

$$iA = \sqrt{2p_0^- 2p_0'^-} Q_q^2 (-ie)^2 \int dx \int dy \text{Tr}[\hat{\varepsilon}_1 G(x-y) \hat{\varepsilon}_2 G(y-x)] e^{-ip_\gamma x + ip_\gamma' y} \quad (\text{C.8})$$

$$\begin{aligned} &= \frac{8\alpha Q_q^2 p_\gamma^+}{\pi} \delta(p_\gamma'^+ - p_\gamma^+) \int dx Q^2 x^2 \bar{x}^2 K_0(r_{12} \sqrt{x\bar{x}Q_\gamma^2}) K_0(r_{12} \sqrt{x\bar{x}Q_\gamma'^2}) \\ &\times \sqrt{2p_0^- 2p_0'^-} \int d^{D-2} r_{2\perp} \int d^{D-2} r_{1\perp} \langle P'(p_0') | T(\text{Tr}[U_1 U_2^\dagger] - N_c) | P(p_0) \rangle. \end{aligned} \quad (\text{C.9})$$

Extracting the dependence on the overall momentum transfer

$$\begin{aligned} \langle P'(p_0') | T \text{Tr}[U_1 U_2^\dagger] | P(p_0) \rangle &= \langle p_0' | e^{\pm i\hat{P} \frac{(r_1+r_2)}{2}} T \text{Tr}[U_{r_1} U_{r_2}^\dagger] e^{\mp i\hat{P} \frac{(r_1+r_2)}{2}} | p_0 \rangle \\ &= e^{ip_{0'0\perp} \frac{(r_1+r_2)_\perp}{2}} \langle p_0' | T \text{Tr}[U_{\frac{r_{12\perp}}{2}} U_{-\frac{r_{12\perp}}{2}}^\dagger] | p_0 \rangle, \end{aligned} \quad (\text{C.10})$$

we get

$$\begin{aligned} iA &= (2\pi)^4 \delta(p_\gamma'^+ - p_\gamma^+) \delta(p_{0'0\perp}) \delta(p_{00'}^-) \int d^2 z \frac{\langle P'(p_0') | T(\text{Tr}[U_{\frac{z}{2}} U_{-\frac{z}{2}}^\dagger] - N_c) | P(p_0) \rangle}{2\pi \delta(p_{00'}^-)} \\ &\times \sqrt{2p_0^- 2p_0'^-} \frac{4\alpha Q_q^2 p_\gamma^+}{\pi^2} \int dx Q^2 x^2 \bar{x}^2 K_0(z \sqrt{x\bar{x}Q_\gamma^2}) K_0(z \sqrt{x\bar{x}Q_\gamma'^2}). \end{aligned} \quad (\text{C.11})$$

Then, using the optical theorem

$$\begin{aligned} \sigma_{tot} &= \frac{\text{Im} A_{ii}}{2s} = \int d^2 z \frac{\langle P'(p_0') | T(\text{Tr}[U_{\frac{z}{2}} U_{-\frac{z}{2}}^\dagger] - N_c) | P(p_0) \rangle}{2\pi \delta(p_{00'}^-)} \Bigg|_{p_0' \rightarrow p_0} \\ &\times \frac{\alpha Q_q^2}{2\pi^2} \int dx 4Q^2 x^2 \bar{x}^2 K_0^2(z \sqrt{x\bar{x}Q_\gamma^2}). \end{aligned} \quad (\text{C.12})$$

Comparing this result to eqs. (3.7–9) in ref. [42], we get the same result (C.7) for F as before.

References

- [1] H1 collaboration, *Diffractive deep-inelastic scattering with a leading proton at HERA*, *Eur. Phys. J.* **C48** (2006) 749 [[hep-ex/0606003](#)].
- [2] H1 collaboration, *Measurement and QCD analysis of the diffractive deep-inelastic scattering cross-section at HERA*, *Eur. Phys. J.* **C48** (2006) 715 [[hep-ex/0606004](#)].
- [3] ZEUS COLLABORATION collaboration, *Dissociation of virtual photons in events with a leading proton at HERA*, *Eur. Phys. J.* **C38** (2004) 43 [[hep-ex/0408009](#)].
- [4] ZEUS collaboration, *Study of deep inelastic inclusive and diffractive scattering with the ZEUS forward plug calorimeter*, *Nucl. Phys.* **B713** (2005) 3 [[hep-ex/0501060](#)].

- [5] F. Aaron, C. Alexa, V. Andreev, S. Backovic, A. Baghdasaryan et al., *Measurement of the cross section for diffractive deep-inelastic scattering with a leading proton at HERA*, *Eur. Phys. J.* **C71** (2011) 1578 [1010.1476].
- [6] H1 COLLABORATION collaboration, *Inclusive Measurement of Diffractive Deep-Inelastic Scattering at HERA*, *Eur. Phys. J.* **C72** (2012) 2074 [1203.4495].
- [7] ZEUS COLLABORATION collaboration, *Deep inelastic scattering with leading protons or large rapidity gaps at HERA*, *Nucl. Phys.* **B816** (2009) 1 [0812.2003].
- [8] H1 COLLABORATION, ZEUS COLLABORATION collaboration, *Combined inclusive diffractive cross sections measured with forward proton spectrometers in deep inelastic ep scattering at HERA*, *Eur. Phys. J.* **C72** (2012) 2175 [1207.4864].
- [9] J. C. Collins, *Proof of factorization for diffractive hard scattering*, *Phys. Rev.* **D57** (1998) 3051 [hep-ph/9709499].
- [10] V. Guzey and M. Klasen, *Diffractive dijet photoproduction in ultraperipheral collisions at the LHC in next-to-leading order QCD*, *JHEP* **04** (2016) 158 [1603.06055].
- [11] V. Guzey and M. Klasen, *A fresh look at factorization breaking in diffractive photoproduction of dijets at HERA at next-to-leading order QCD*, *Eur. Phys. J.* **C76** (2016) 467 [1606.01350].
- [12] V. Guzey and M. Klasen, *Inclusive dijet photoproduction in ultraperipheral heavy-ion collisions at the LHC in next-to-leading order QCD*, 1811.10236.
- [13] V. Guzey and M. Klasen, *Constraints on nuclear parton distributions from dijet photoproduction at the LHC*, *Eur. Phys. J.* **C79** (2019) 396 [1902.05126].
- [14] J. Bartels, J. R. Ellis, H. Kowalski and M. Wüsthoff, *An analysis of diffraction in deep-inelastic scattering*, *Eur. Phys. J.* **C7** (1999) 443 [hep-ph/9803497].
- [15] ZEUS collaboration, *Production of exclusive dijets in diffractive deep inelastic scattering at HERA*, *Eur. Phys. J.* **C76** (2016) 16 [1505.05783].
- [16] J. Bartels, C. Ewerz, H. Lotter and M. Wüsthoff, *Azimuthal distribution of quark - anti-quark jets in DIS diffractive dissociation*, *Phys. Lett.* **B386** (1996) 389 [hep-ph/9605356].
- [17] R. Boussarie, A. Grabovsky, L. Szymanowski and S. Wallon, *Impact factor for high-energy two and three jets diffractive production*, *JHEP* **1409** (2014) 026 [1405.7676].
- [18] R. Boussarie, A. V. Grabovsky, L. Szymanowski and S. Wallon, *On the one loop $\gamma^{(*)} \rightarrow q\bar{q}$ impact factor and the exclusive diffractive cross sections for the production of two or three jets*, *JHEP* **11** (2016) 149 [1606.00419].
- [19] R. Boussarie, A. V. Grabovsky, D. Yu. Ivanov, L. Szymanowski and S. Wallon, *Next-to-Leading Order Computation of Exclusive Diffractive Light Vector Meson Production in a Saturation Framework*, *Phys. Rev. Lett.* **119** (2017) 072002 [1612.08026].
- [20] I. Balitsky, *Operator expansion for high-energy scattering*, *Nucl. Phys.* **B463** (1996) 99 [hep-ph/9509348].
- [21] I. Balitsky, *Factorization for high-energy scattering*, *Phys. Rev. Lett.* **81** (1998) 2024 [hep-ph/9807434].
- [22] I. Balitsky, *Factorization and high-energy effective action*, *Phys. Rev.* **D60** (1999) 014020 [hep-ph/9812311].

- [23] I. Balitsky, *Effective field theory for the small- x evolution*, *Phys. Lett.* **B518** (2001) 235 [[hep-ph/0105334](#)].
- [24] J. Jalilian-Marian, A. Kovner, A. Leonidov and H. Weigert, *The BFKL equation from the Wilson renormalization group*, *Nucl. Phys.* **B504** (1997) 415 [[hep-ph/9701284](#)].
- [25] J. Jalilian-Marian, A. Kovner, A. Leonidov and H. Weigert, *The Wilson renormalization group for low x physics: Towards the high density regime*, *Phys. Rev.* **D59** (1999) 014014 [[hep-ph/9706377](#)].
- [26] J. Jalilian-Marian, A. Kovner and H. Weigert, *The Wilson renormalization group for low x physics: Gluon evolution at finite parton density*, *Phys. Rev.* **D59** (1999) 014015 [[hep-ph/9709432](#)].
- [27] J. Jalilian-Marian, A. Kovner, A. Leonidov and H. Weigert, *Unitarization of gluon distribution in the doubly logarithmic regime at high density*, *Phys. Rev.* **D59** (1999) 034007 [[hep-ph/9807462](#)].
- [28] A. Kovner, J. G. Milhano and H. Weigert, *Relating different approaches to nonlinear QCD evolution at finite gluon density*, *Phys. Rev.* **D62** (2000) 114005 [[hep-ph/0004014](#)].
- [29] H. Weigert, *Unitarity at small Bjorken x* , *Nucl. Phys.* **A703** (2002) 823 [[hep-ph/0004044](#)].
- [30] E. Iancu, A. Leonidov and L. D. McLerran, *Nonlinear gluon evolution in the color glass condensate. I*, *Nucl. Phys.* **A692** (2001) 583 [[hep-ph/0011241](#)].
- [31] E. Iancu, A. Leonidov and L. D. McLerran, *The renormalization group equation for the color glass condensate*, *Phys. Lett.* **B510** (2001) 133 [[hep-ph/0102009](#)].
- [32] E. Ferreira, E. Iancu, A. Leonidov and L. McLerran, *Nonlinear gluon evolution in the color glass condensate. II*, *Nucl. Phys.* **A703** (2002) 489 [[hep-ph/0109115](#)].
- [33] Y. Hatta, B.-W. Xiao and F. Yuan, *Probing the Small- x Gluon Tomography in Correlated Hard Diffractive Dijet Production in DIS*, *Phys. Rev. Lett.* **116** (2016) 202301 [[1601.01585](#)].
- [34] T. Altinoluk, N. Armesto, G. Beuf and A. H. Rezaeian, *Diffractive Dijet Production in Deep Inelastic Scattering and Photon-Hadron Collisions in the Color Glass Condensate*, *Phys. Lett.* **B758** (2016) 373 [[1511.07452](#)].
- [35] H. Mäntysaari, N. Mueller and B. Schenke, *Diffractive Dijet Production and Wigner Distributions from the Color Glass Condensate*, *Phys. Rev.* **D99** (2019) 074004 [[1902.05087](#)].
- [36] F. Salazar and B. Schenke, *Diffractive dijet production in impact parameter dependent saturation models*, [1905.03763](#).
- [37] Y. Hagiwara, Y. Hatta, R. Pasechnik, M. Tasevsky and O. Teryaev, *Accessing the gluon Wigner distribution in ultraperipheral pA collisions*, *Phys. Rev.* **D96** (2017) 034009 [[1706.01765](#)].
- [38] E. Iancu and A. H. Rezaeian, *Elliptic flow from color-dipole orientation in pp and pA collisions*, *Phys. Rev.* **D95** (2017) 094003 [[1702.03943](#)].
- [39] Y. Hagiwara, Y. Hatta, B.-W. Xiao and F. Yuan, *Elliptic Flow in Small Systems due to Elliptic Gluon Distributions?*, *Phys. Lett.* **B771** (2017) 374 [[1701.04254](#)].
- [40] X. Ji, F. Yuan and Y. Zhao, *Hunting the Gluon Orbital Angular Momentum at the Electron-Ion Collider*, *Phys. Rev. Lett.* **118** (2017) 192004 [[1612.02438](#)].

- [41] Y. Hatta, Y. Nakagawa, F. Yuan, Y. Zhao and B. Xiao, *Gluon orbital angular momentum at small- x* , *Phys. Rev.* **D95** (2017) 114032 [[1612.02445](#)].
- [42] K. J. Golec-Biernat, *Deep Inelastic Scattering at Small Values of the Bjorken Variable x* , Habilitation thesis, Krakow/Hamburg, 2001.
- [43] N. Brown and W. J. Stirling, *Finding jets and summing soft gluons: A New algorithm*, *Z. Phys.* **C53** (1992) 629.
- [44] S. Catani, Y. L. Dokshitzer, M. Olsson, G. Turnock and B. R. Webber, *New clustering algorithm for multi - jet cross-sections in $e+ e-$ annihilation*, *Phys. Lett.* **B269** (1991) 432.
- [45] K. Golec-Biernat and M. Wüsthoff, *Saturation effects in deep inelastic scattering at low Q^2 and its implications on diffraction*, *Phys. Rev.* **D59** (1999) 014017 [[hep-ph/9807513](#)].
- [46] H. Kowalski, L. Motyka and G. Watt, *Exclusive diffractive processes at HERA within the dipole picture*, *Phys. Rev.* **D74** (2006) 074016 [[hep-ph/0606272](#)].